RECOMMENDED PRACTICE
DNV-RP-F105

FREE SPANNING PIPELINES

FEBRUARY 2006

DET NORSKE VERITAS

FOREWORD

DET NORSKE VERITAS (DNV) is an autonomous and independent foundation with the objectives of safeguarding life, property and the environment, at sea and onshore. DNV undertakes classification, certification, and other verification and consultancy services relating to quality of ships, offshore units and installations, and onshore industries worldwide, and carries out research in relation to these functions.

DNV Offshore Codes consist of a three level hierarchy of documents:

— *Offshore Service Specifications.* Provide principles and procedures of DNV classification, certification, verification and consultancy services.
— *Offshore Standards.* Provide technical provisions and acceptance criteria for general use by the offshore industry as well as the technical basis for DNV offshore services.
— *Recommended Practices.* Provide proven technology and sound engineering practice as well as guidance for the higher level Offshore Service Specifications and Offshore Standards.

DNV Offshore Codes are offered within the following areas:

A) Qualification, Quality and Safety Methodology

B) Materials Technology

C) Structures

D) Systems

E) Special Facilities

F) Pipelines and Risers

G) Asset Operation

H) Marine Operations

J) Wind Turbines

Amendments and Corrections

This document is valid until superseded by a new revision. Minor amendments and corrections will be published in a separate document normally updated twice per year (April and October).

For a complete listing of the changes, see the "Amendments and Corrections" document located at:
http://www.dnv.com/technologyservices/, "Offshore Rules & Standards", "Viewing Area".

The electronic web-versions of the DNV Offshore Codes will be regularly updated to include these amendments and corrections.

Comments may be sent by e-mail to *rules@dnv.com*
For subscription orders or information about subscription terms, please use *distribution@dnv.com*
Comprehensive information about DNV services, research and publications can be found at *http*://www.dnv.com, or can be obtained from DNV, Veritasveien 1, NO-1322 Høvik, Norway; Tel +47 67 57 99 00, Fax +47 67 57 99 11.

Computer Typesetting (FM+SGML) by Det Norske Veritas.
Printed in Norway

Relationship to Rules under preparation

Parts of this Recommended Practice should be read in conjunction with the following two documents:

— DNV-RP-F110 "Global Buckling of Pipelines", and
— DNV-RP-C205 - "Environmental Conditions and Environmental Loads".

However, these two documents are currently under preparation at DNV.

Readers are requested to contact:

RP-F110: Leif Collberg, TNCNO714, Det Norske Veritas, Veritasveien 1, N-1322 Høvik,
mailto: Leif.Collberg@dnv.com

RP-C205: Arne Nestegaard, TNCNO785, Det Norske Veritas, Veritasveien 1, N-1322 Høvik,
mailto: Arne.Nestegard@dnv.com

for more information, if required.

Motives

The existing design code, DNV-RP-F105 for "Free Spanning Pipelines" from March 2002, can be effectively applied to deal with both single and multiple spans vibrating predominantly in a single mode. In the case where there is a combination of long spans and high currents, not only does the fundamental eigen modes become activated, but also the higher modes. Such a multimode response is not prohibited by the design code. However, no detailed guidance is provided in the present Recommended Practice (RP) about the fatigue damage from multimode vibrations.

During the Ormen Lange project a strong focus was put on design procedures for long free spans in order to make this project feasible and in order to save seabed intervention costs. A relatively large R&D project on free span vortex-induced vibrations (VIV) was performed. The results of this project was synthesised into a project specific guideline issued by DNV, concerning the calculation procedures and design acceptance criteria for long free span with multi-mode response.

The main objective of this proposal is to include the experiences gained from the Ormen Lange Project regarding multi-mode and multi-span response and incorporate the latest R&D work relating to Free Spanning Pipelines. This proposal has been worked out through a JIP with Hydro and Statoil. In addition to the multi-mode response aspects, a general update and revision of the DNV-RP-F105 has been performed, based on feedback and experience from several projects and users.

Main changes

The most important changes in this update are:

— Computational procedure for multi-mode analysis, selection of vibration modes and combination of stresses.
— Guidance on mitigation measures for vortex-induced vibrations.
— Ultimate limit state criteria (over-stress) updated.
— Recalibrated safety factors.
— Detailed calculation procedure for pipe-soil interaction.
— Practical guidance on various aspects based on project experience from several sources.
— Update of response models for vortex-induced vibrations based on available test results.
— Clarified limitations and range of application.
— Added mass modification during cross-flow vibrations.

This update strengthens the position of this RP as the state-of-the-art document for free spanning pipelines. It allows longer spans to be accepted as detailed calculation procedures for multiple mode response is given.

Acknowledgement:

The following companies are gratefully acknowledged for their contributions to this Recommended Practice:

DHI
Hydro
Reinertsen
Statoil
Snamprogetti

DNV is grateful for the valuable co-operations and discussions with the individual personnel of these companies.

The multispan and multi-mode studies were funded by the Ormen Lange license group.
Hydro and its license partners BP, Exxon, Petoro, Shell and Statoil are acknowledged for the permission to use these results.

CONTENTS

1. General

1.1 Introduction

1.1.1 The present document considers free spanning pipelines subjected to combined wave and current loading. The premises for the document are based on technical development within pipeline free span technology in recent R&D projects, as well as design experience from recent and ongoing projects, i.e.:

— DNV Guideline 14, see Mørk & Fyrileiv (1998).
— The sections regarding Geotechnical Conditions and part of the hydrodynamic model are based on the research performed in the GUDESP project, see Tura et al. (1994).
— The sections regarding Free Span Analysis and in-line Vortex Induced Vibrations (VIV) fatigue analyses are based on the published results from the MULTISPAN project, see Mørk et al. (1997).
— Numerical study based on CFD simulations for vibrations of a pipeline in the vicinity of a trench, performed by Statoil, DHI & DNV, see Hansen et al. (2001).
— Further, recent R&D and design experience e.g. from Åsgard Transport, ZEEPIPE, TOGI and TROLL OIL pipeline projects are implemented, see Fyrileiv et al. (2005).
— Ormen Lange tests aimed at moderate and very long spans with multimodal behaviour, see Fyrileiv et al. (2004), Chezhian et al. (2003) and Mørk et al. (2003).

The basic principles applied in this document are in agreement with most recognised rules and reflect state-of-the-art industry practice and latest research.

This document includes a brief introduction to the basic hydrodynamic phenomena, principles and parameters. For a thorough introduction see e.g. Sumer & Fredsøe (1997) and Blevins (1994).

1.2 Objective

1.2.1 The objective of this document is to provide rational design criteria and guidance for assessment of pipeline free spans subjected to combined wave and current loading.

1.3 Scope and application

1.3.1 Detailed design criteria are specified for Ultimate Limit State (ULS) and Fatigue Limit State (FLS) due to in-line and cross-flow Vortex Induced Vibrations (VIV) and direct wave loading.

The following topics are considered:

— methodologies for free span analysis
— requirements for structural modelling
— geotechnical conditions
— environmental conditions and loads
— requirements for fatigue analysis
— VIV response and direct wave force analysis models
— acceptance criteria.

1.3.2 Free spans can be caused by:

— seabed unevenness
— change of seabed topology (e.g. scouring, sand waves)
— artificial supports/rock beams etc.
— strudel scours.

1.3.3 The following environmental flow conditions are described in this document:

— steady flow due to current
— oscillatory flow due to waves
— combined flow due to current and waves.

The flow regimes are discussed in 1.9.

1.3.4 This Recommended Practice is strictly speaking only applicable for circular pipe cross-section of steel pipelines. However, it can be applied with care to non-circular cross-sections such as piggy-back solutions as long as other hydrodynamic loading phenomena, e.g. galloping, are properly taken into account.

Basic principles may also be applied to more complex cross sections such as pipe-in-pipe, bundles, flexible pipes and umbilicals.

1.3.5 There are no limitations to span length and span gap with respect to application of this Recommended Practice.

Both single spans and multiple spans scenarios, either in single mode or multiple mode vibration, can be assessed using this RP.

Unless otherwise documented, the damage contribution for different modes should relate to the same critical (weld) location along the span.

1.3.6 The free span analysis may be based on approximate response expressions or a refined FE approach depending on the free span classification and response type, see Sec.6.

The following cases are considered:

— single spans
— spans interacting with adjacent/side spans.

The stress ranges and natural frequencies should normally be obtained from an FE-approach. Requirements to the structural modelling and free span analyses are given in Sec.6.

1.3.7 The following models are considered:

— response models (RM)
— force models (FM).

An amplitude response model is applicable when the vibration of the free span is dominated by vortex induced resonance phenomena. A force model (Morison's equation) may be used when the free span dominated by hydrodynamic loads such as direct wave loads. The selection of an appropriate model may be based on the prevailing flow regimes, see 1.9.

1.3.8 The fatigue criterion is limited to stress cycles within the elastic range. Low cycle fatigue due to elasto-plastic behaviour is considered outside the scope of this document.

1.3.9 Fatigue loads due to trawl interaction, cyclic loads during installation or pressure variations are not considered herein but must be considered as a part of the integrated fatigue damage assessment.

1.3.10 Procedures and criteria for structural design or assessment of free spanning HT/HP pipelines have not been included within the scope of this Recommended Practice.

Free spans due to uplift are however within the scope of this document.

Note:

For information concerning a reference document (currently in preparation), regarding procedures and criteria for structural design or assessment of HP/HT pipelines, contact TNCNO714, DNV, Høvik, Norway.

1.3.11 The main aspects of a free span assessment together with key parameters and main results are illustrated in the figure below.

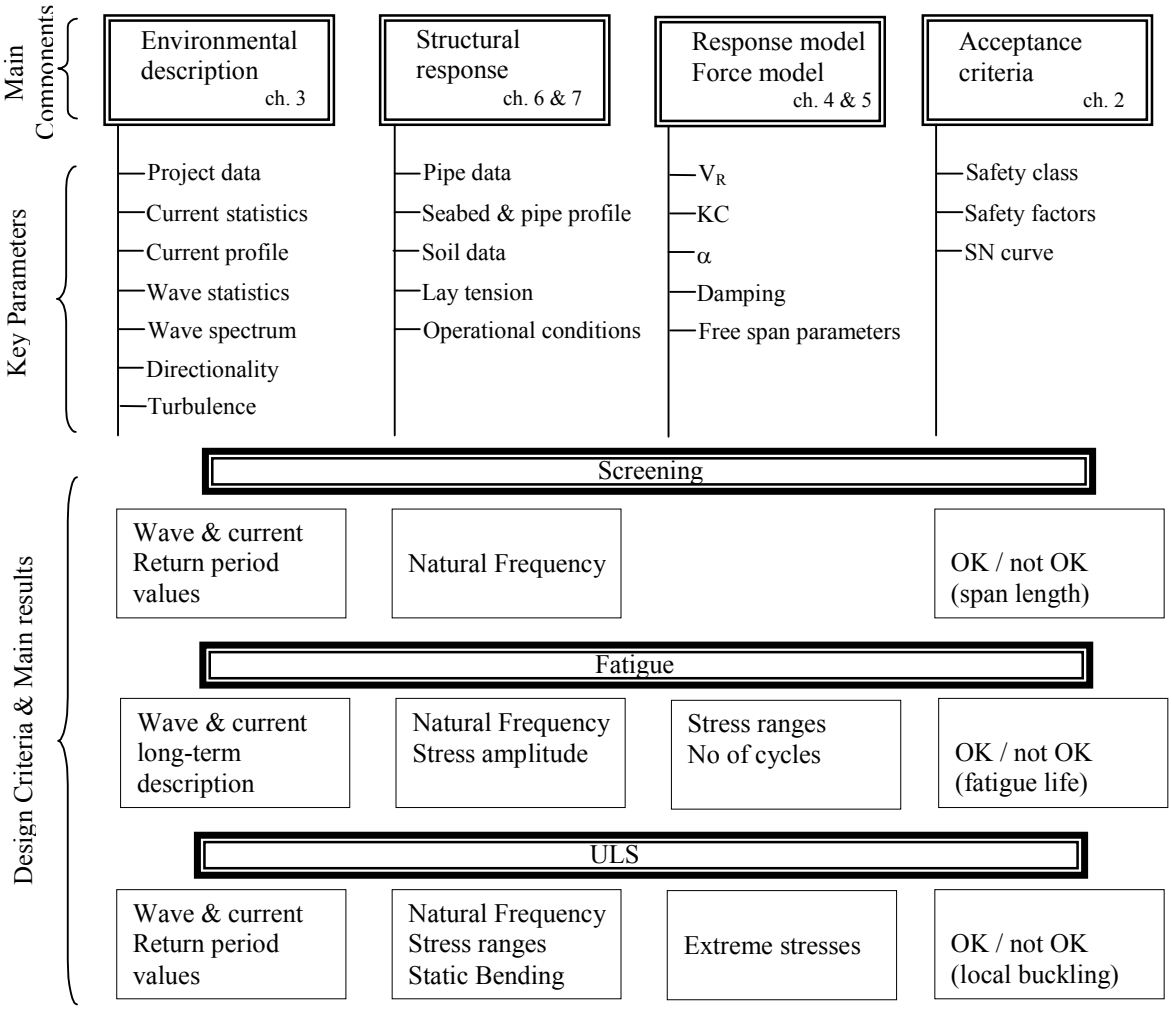

Figure 1-1
Overview of main components in a free span assessment

1.4 Extending the application scope of this RP

1.4.1 The primary focus of this RP is on free spanning subsea pipelines.

1.4.2 The fundamental principles given in this RP may also be applied and extended to other offshore elements such as cylindrical structural elements of the jackets, risers from fixed platforms etc., at the designer's discretion. However some limitations apply and these are discussed in Appendix C, C.2.

1.4.3 For a more detailed account of riser VIV, reference is made to the DNV-RP-F204 "Riser Fatigue".

1.5 Safety philosophy

1.5.1 The safety philosophy adopted herein complies with Sec.2 in DNV-OS-F101.

1.5.2 The reliability of the pipeline against failure is ensured by use of a Load and Resistance Factors Design Format (LRFD).

— For the in-line and cross-flow VIV acceptance criterion, the set of safety factors is calibrated to acceptable target reliability levels using reliability-based methods.
— For all other acceptance criteria, the recommended safety factors are based on engineering judgement in order to obtain a safety level equivalent to modern industry practice.
— Use of case specific safety factors based on quantification of uncertainty in fatigue damage, can also be considered.

1.6 Free span morphological classification

1.6.1 The objective of the morphological classification is to define whether the free span is isolated or interacting. The morphological classification determines the degree of complexity required of the free span analysis:

— Two or more consecutive free spans are considered to be isolated (i.e. single span) if the static and dynamic behaviour is unaffected by neighbouring spans.
— A sequence of free spans is interacting (i.e. multi-spanning) if the static and dynamic behaviour is affected by the presence of neighbouring spans. If the free span is interacting, more than one span must be included in the pipe/seabed model.

1.6.2 The classification may be useful in the following cases:

— for evaluating multi-mode response of single and multi-spans
— for evaluation of scour induced free spans and in application of approximate response quantities described in Sec.6.7.

1.6.3 The morphological classification should in general be determined based on detailed static and dynamic analyses.

Guidance note:

When long segments of the pipeline are analysed in automated FE analysis tools, certain limitations can arise for identifying interacting spans.

The following example illustrates the same:

Two free spans which are separated by a distance of 1000 m and each with a span length of about 50 m. The FE analysis estimates that some of the response frequencies for these two spans are identical. Further, due to numerical approximations or due to round off errors, the results may be presented as single mode response at these two spans, i.e. it is a single interacting mode at these two spans.

However, in reality these two spans are physically separated by a considerable distance, and not interacting.

If isolated spans are incorrectly modelled as interacting multispans, it may also lead to significant errors in estimating the fatigue damage. The fatigue damage is dependent on the unit stress amplitudes, as discussed in Sec.4. The unit stress amplitudes are dependent on the normalised mode shape, which is related to the span length over which the normalisation is considered. When long multispans are analysed, the normalisation will not be same as for an isolated single span, within the multi-spanning system. This will in turn lead to errors.

Experience has shown that in case of close frequencies for spans, the FE analysis may predict interaction even though the physical distance between the spans is quite long. In case of mode shapes with deflection in spans that seem to be physically well separated, use of appropriate axial pipe-soil stiffness and/or local restraints in between the spans should be considered to separate individual modes.

Hence, caution should be exercised when using automated FE tools for identifying interacting spans.

---e-n-d---of---G-u-i-d-a-n-c-e---n-o-t-e---

1.6.4 In lieu of detailed data, Figure 1-2 may be used to classify spans into isolated or interacting depending on soil types and span/span support lengths. Figure 1-2 is provided only for indicative purposes and is applicable only for horizontal supports. The curves are, in strict terms, only valid for the vertical (cross-flow) dynamic response but may also be used for assessment of the horizontal (in-line) response.

Note that Figure 1-2 indicates that for a given span scenario the spans will tend to interact more as the soil becomes softer. However, given a seabed profile, a softer soil will tend to have shorter and fewer spans and probably less interacting spans than a harder soil.

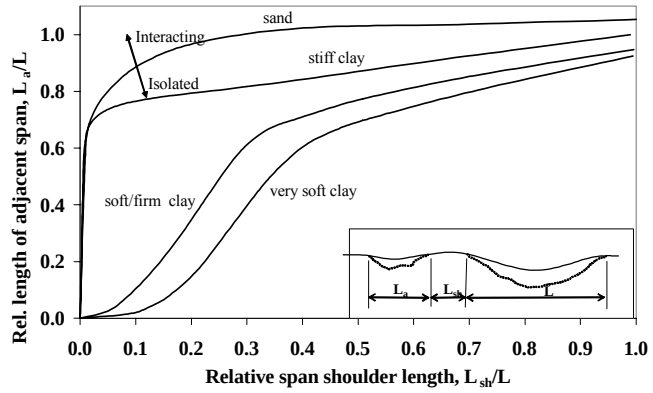

Figure 1-2
Classification of free spans

1.7 Free span response classification

1.7.1 The free spans vibrations can be classified and analysed under the following categories:

— isolated single span - single mode response
— isolated single span - multi-mode response
— interacting multispans - single mode response
— interacting multispans - multi-mode response.

1.7.2 In case several vibration modes (in the same direction) may become active at a given flow velocity, multi-mode response shall be considered.

1.7.3 The following, simple and conservative procedure can be used to check for single or multi-mode response:

— Establish the lowest frequencies in both vertical (cross-flow) and horizontal (in-line) direction for the free span to be considered.
— Identify frequencies that may be excited by applying the following simplified criterion:

$V_{Rd,CF} > 2$ for cross-flow
$V_{Rd,IL} > 1$ for in-line

Here, the reduced velocity may be calculated using the 1-year flow condition at the pipe level, see Sec.3.

— In case only one mode meets this criterion, the response is single mode. If not, the response is multi-mode.

Guidance note:

Normally the in-line and cross-flow frequencies are to be established using FE analysis. The approximate response quantities in Sec.6.7 can be used, if applicable.

---e-n-d---of---G-u-i-d-a-n-c-e---n-o-t-e---

1.8 Free span response behaviour

1.8.1 An overview of typical free span characteristics is given in the table below as a function of the free span length. The ranges indicated for the normalised free span length in terms of (L/D) are tentative and given for illustration only.

Table 1-1

L/D	*Response description*
L/D < 30 [1]	**Very little dynamic amplification.** Normally not required to perform comprehensive fatigue design check. Insignificant dynamic response from environmental loads expected and unlikely to experience VIV.
30 < L/D < 100	**Response dominated by beam behaviour.** Typical span length for operating conditions. Natural frequencies sensitive to boundary conditions (and effective axial force).
100 < L/D < 200	**Response dominated by combined beam and cable behaviour.** Relevant for free spans at uneven seabed in temporary conditions. Natural frequencies sensitive to boundary conditions, effective axial force (including initial deflection, geometric stiffness) and pipe "feed in". Refer to 1.7 for free span response classification, which provides practical guidance for engineering applications, with respect to single and multi-mode response.
L/D > 200	**Response dominated by cable behaviour.** Relevant for small diameter pipes in temporary conditions. Natural frequencies governed by deflected shape and effective axial force.

1) For hot pipelines (response dominated by the effective axial force) or under extreme current conditions ($U_c > 1.0 – 2.0$ m/s) this L/D limit may be misleading.

1.9 Flow regimes

1.9.1 The current flow velocity ratio, $\alpha = U_c/(U_c + U_w)$ (where U_c is the current velocity normal to the pipe and U_w is the significant wave-induced velocity amplitude normal to the pipe, see Sec.4), may be applied to classify the flow regimes as follows:

$\alpha < 0.5$	**wave dominant - wave superimposed by current.** **In-line** direction: in-line loads may be described according to Morison's formulae, see Sec.5. In-line VIV due to vortex shedding is negligible. **Cross-flow** direction: cross-flow loads are mainly due to asymmetric vortex shedding. A response model, see Sec.4, is recommended.
$0.5 < \alpha < 0.8$	**wave dominant – current superimposed by wave.** **In-line** direction: in-line loads may be described according to Morison's formulae, see Sec.5. In-line VIV due to vortex shedding is mitigated due to the presence of waves. **Cross-flow** direction: cross-flow loads are mainly due to asymmetric vortex shedding and resemble the current dominated situation. A response model, see Sec.4, is recommended.
$\alpha > 0.8$	**current dominant** **In-line** direction: in-line loads comprises the following components: — a steady drag dominated component — an oscillatory component due to regular vortex shedding For fatigue analyses a response model applies, see Sec.4. In-line loads according to Morison's formulae are normally negligible. **Cross-flow** direction: cross-flow loads are cyclic and due to vortex shedding and resembles the pure current situation. A response model, see Sec.4, is recommended.

Note that $\alpha = 0$ correspond to pure oscillatory flow due to waves and $\alpha = 1$ corresponds to pure (steady) current flow.

The flow regimes are illustrated in Figure 1-3.

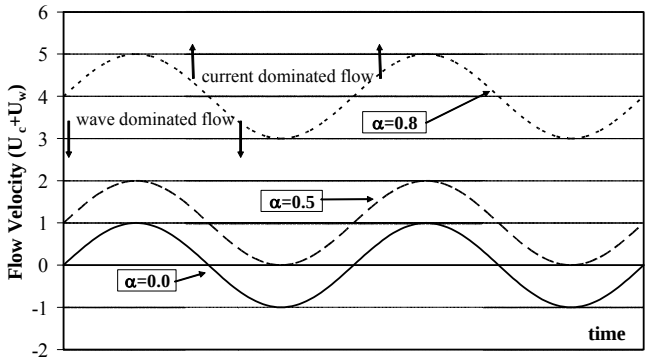

Figure 1-3
Flow regimes

1.9.2 Oscillatory flow due to waves is stochastic in nature, and a random sequence of wave heights and associated wave periods generates a random sequence of near seabed horizontal oscillations. For VIV analyses, the significant velocity amplitude, U_w, is assumed to represent a single sea-state. This is likely to be a conservative approximation.

1.10 VIV assessment methodologies

1.10.1 Different VIV assessment methodologies exists for assessing cross-flow VIV induced fatigue in free spanning pipelines.

1.10.2 This RP applies the so-called Response Models approach to predict the vibration amplitudes due to vortex shedding. These response models are empirical relations between the reduced velocity defined in terms of the still-water natural frequency and the non-dimensional response amplitude. Hence the stress response is derived from an assumed vibration modes with an empirical amplitude response.

1.10.3 Another method is based on semi-empirical lift coefficient curves as a function of vibration amplitude and non-dimensional vibration frequency. By use of the concept of added mass the stress response comes as a direct result from the analysis, see Larsen & Koushan (2005)

Guidance note:

The key difference between these methods is not in the solution strategy, but the basis and validity range for the applied empirical parameters. Further, some tools vary in modelling flexibility and extent of user defined control parameters (bandwidth, selection of Strouhal no., etc.) to estimate fatigue damage.

---e-n-d---of---G-u-i-d-a-n-c-e---n-o-t-e---

1.10.4 As a third option, Computational Fluid Dynamics (CFD) simulation of the turbulent fluid flow around one- or several pipes can in principle be applied for VIV assessment to overcome the inherent limitations of the state-of-practice engineering approach. The application of CFD for VIV assessment is at present severely limited by the computational effort required. In addition, documented work is lacking which shows that the estimated fatigue damage based on CFD for realistic free span scenarios gives better and satisfactory response, than the methods described above.

1.10.5 Particularly for VIV of special pipeline designs (pipe-in-pipe, bundled pipelines, piggy back pipelines, etc.) with limited experience, experiments should be considered. Experiments should also be performed when considering pipelines which use new designs for VIV mitigation devices.

1.10.6 Circular and complex cross-sections such as pipe-in-pipe and bundles may be treated as an ordinary pipe as long as changes in structural response, damping and fatigue properties are accounted for.

1.10.7 Non-circular bluff-body cross-sections such as piggy back solutions may be considered by applying a larger hydrodynamic diameter and considering the most critical cross-sectional orientation in the calculations.

1.11 Relationship to other Rules

1.11.1 This document formally supports and complies with the DNV Offshore Standard "Submarine Pipeline Systems", DNV-OS-F101, 2000 and is considered to be a supplement to relevant National Rules and Regulations.

1.11.2 This document is supported by other DNV offshore codes as follows:

— Recommended Practice DNV-RP-C203 "Fatigue Strength Analysis of Offshore Steel Structures"
— Offshore Standard DNV-OS-F201 "Dynamic Risers"
— Recommended Practice DNV-RP-F204 "Riser Fatigue".

In case of conflict between requirements of this RP and a referenced DNV Offshore Code, the requirements of the code with the latest revision date shall prevail.

Guidance note:

Any conflict is intended to be removed in next revision of that document.

---e-n-d---of---G-u-i-d-a-n-c-e---n-o-t-e---

In case of conflict between requirements of this RP and a non DNV referenced document, the requirements of this RP shall prevail.

1.12 Definitions

1.12.1 *Effective Span Length* is the length of an idealised fixed-fixed span having the same structural response in terms of natural frequencies as the real free span supported on soil.

1.12.2 *Force Model* is in this document a model where the environmental load is based on Morison's force expression.

1.12.3 *Gap* is defined as the distance between the pipe and the seabed. The gap used in design, as a single representative value, must be characteristic for the free span

The gap may be calculated as the average value over the central third of the span.

1.12.4 *Marginal Fatigue Capacity* is defined as the fatigue capacity (life) with respect to one sea state defined by its significant wave height, peak period and direction.

1.12.5 *Multi-mode Response*, denotes response for a span where several vibration modes may be excited simultaneously in the same direction (in-line or cross-flow).

1.12.6 *Multi-spans* are spans where the adjacent spans have a influence on the behaviour and response of a span.

1.12.7 *Non-stationary Span* is a span where the main span characteristics such as span length and gap change significantly over the design life, e.g. due to scouring of the seabed.

1.12.8 *Response Model* is a model where the structural response due to VIV is determined by hydrodynamic parameters.

1.12.9 *Span Length* is defined as the length where a continuous gap exists, i.e. as the visual span length.

1.12.10 *Single Span* is a span which is an isolated span that can be assessed independent of the neighbouring spans.

1.12.11 *Stationary Span* is a span where the main span characteristics such as span length and gap remain the same over the design life.

1.13 Abbreviations

CF	cross-flow
CSF	concrete stiffness factor
FLS	fatigue limit state
FM	force model
IL	in-line
LRFD	load and resistance factors design format
OCR	over-consolidation ratio (only clays)
RM	response model (VIV)
RD	response domain
RPV	return period values
SRSS	square root of the sum of squares
TD	time domain
ULS	ultimate limit state
VIV	vortex induced vibrations

1.14 Symbols

1.14.1 Latin

a_κ	parameter for rain-flow counting factor
$\bar{a}$	characteristic fatigue strength constant
A_e	external cross-section area
A_i	internal cross-section (bore) area
A_{IL}	in-line unit amplitude stress (stress induced by a pipe (vibration mode) deflection equal to an outer diameter D)
A_{CF}	cross-flow unit amplitude stress
A_p	cross sectional area of penetrated pipe
A_s	pipe steel cross section area
(A_Y/D)	normalised in-line VIV amplitude
(A_Z/D)	normalised cross-flow VIV amplitude
b	linearisation constant
B	pipe-soil contact width
b_κ	parameter for rain flow counting factor
C_a	added mass coefficient (C_M-1)
$C_{a,\ CF\text{-}RES}$	added mass coefficient due to cross-flow response
C_D	drag coefficient
C_D^0	basic drag coefficient
C_M	the inertia coefficient
C_M^0	basic inertia coefficient
C_L	coefficient for lateral soil stiffness
C_V	coefficient for vertical soil stiffness
C_T	constant for long-term wave period distribution
$C_{1\text{-}6}$	Boundary condition coefficients
c(s)	soil damping per unit length
d	trench depth
D	pipe outer diameter (including any coating)
D_{fat}	deterministic fatigue damage
D_s	outer steel diameter
E	Young's modulus
EI	bending stiffness
e	seabed gap
e_s	void ratio
(e/D)	seabed gap ratio
f_{cyc}	frequency used for fatigue stress cycle counting in case of multimode response
f_c	frequency used for fatigue stress cycle counting in case of multimode response
f_n	n'th eigen frequency of span in-line ($f_{n,IL}$) or cross-flow ($f_{n,CF}$) natural frequency (determined at no flow around the pipe)
f_{cn}	concrete construction strength
f_s	vortex shedding frequency

$$(\text{Strouhal frequency}) = S_t \frac{U}{D}$$

F	correction factor for pipe roughness
F_L	lateral pipe-soil contact force
F_V	vertical pipe-soil contact force
f_v	dominating vibration frequency
f_w	wave frequency
F()	distribution function
F_X	cumulative distribution function
g	acceleration of gravity
g_c	correction function due to steady current
g_D	drag force term
g_I	inertia force term
G	shear modulus of soil or incomplete complementary Gamma function

$G(\omega)$	frequency transfer function from wave elevation to flow velocity
H_{eff}	effective lay tension
H_S	significant wave height
h	water depth, i.e. distance from the mean sea level to the pipe
I	moment of inertia
I_c	turbulence intensity over 30 minutes
I_p	plasticity index, cohesive soils
k	wave number or depth gradient
k_c	soil parameter or empirical constant for concrete stiffening
k_m	non-linear factor for drag loading
k_p	peak factor
k_w	normalisation constant
K	soil stiffness
K_L	lateral (horizontal) dynamic soil stiffness
K_V	vertical dynamic soil stiffness
(k/D)	pipe roughness
KC	Keulegan Carpenter number $= \frac{U_w}{f_w D}$
K_S	stability parameter $= \frac{4\pi m_e \zeta_T}{\rho D^2}$
k_1	soil stiffness
k_2	soil stiffness
L	free span length, (apparent, visual)
L_a	length of adjacent span
L_{eff}	effective span length
L_s	span length with vortex shedding loads
L_{sh}	length of span shoulder
m_e	effective mass per unit length
m	fatigue exponent
m(s)	mass per unit length including structural mass, added mass and mass of internal fluid
M_E	bending moment due to environmental effects
M_{static}	static bending moment
M_n	spectral moments of order n
n_i	number of stress cycles for stress block i
N	number of independent events in a return period
N_i	number of cycles to failure for stress block i
N_{tr}	true steel wall axial force
N_c	soil bearing capacity parameter
N_q	soil bearing capacity parameter
N_{sw}	number of cycles when SN curve change slope
N_γ	soil bearing capacity parameter
p_e	external pressure
p_i	internal pressure
P_i	probability of occurrence for i'th stress cycle
q	deflection load per unit length
P_{cr}	critical buckling load $(1 + CSF)C_2\pi^2 EI/L_{eff}^2$
R_c	current reduction factor
R_D	reduction factor from wave direction and spreading
R_v	vertical soil reaction
$R_{I\theta}$	reduction factor from turbulence and flow direction
R_k	reduction factor from damping
Re	Reynolds number $D = \frac{UD}{\nu}$
s	spreading parameter
S	stress range, i.e. double stress amplitude
S_{comb}	combined stress in case of multi-mode response
S_{sw}	stress at intersection between two SN-curves
S_{eff}	effective axial force
$S_{\eta\eta}$	wave spectral density
S_{SS}	stress spectra
S_{UU}	wave velocity spectra at pipe level
s_u	undrained shear strength, cohesive soils
S_t	Strouhal number
t	pipe wall thickness or time
$T_{exposure}$	load exposure time
T_{life}	fatigue design life capacity
T_p	peak period
T_u	mean zero up-crossing period of oscillating flow
T_w	wave period
U	current velocity
U_c	current velocity normal to the pipe
U_s	significant wave velocity
U_w	significant wave-induced flow velocity normal to the pipe, corrected for wave direction and spreading
v	vertical soil settlement (pipe embedment)
V_R	reduced velocity $= \frac{U_c + U_w}{f_n D}$
V_{Rd}	reduced velocity (design value) with safety factor $= V_{R\gamma f}$
w	wave energy spreading function
y	lateral pipe displacement
z	height above seabed or in-line pipe displacement
z_m	macro roughness parameter
z_0	sea-bottom roughness
z_r	reference (measurement) height

1.14.2 Greek

α	current flow velocity ratio, generalised Phillips' constant or Weibull scale parameter
α_j	reduction factor for in-line mode, j
α_e	temperature expansion coefficient
α_{fat}	Allowable fatigue damage ratio according to DNV OS-F101
α_T	parameter to determine wave period
β	Weibull shape parameter and relative soil stiffness parameter
Δ/D	relative trench depth
Δp_i	internal pressure difference relative to laying
ΔT	temperature difference relative to laying or storm duration

δ	pipe deflection or statistical skewness
ε	band-width parameter
Γ	gamma function
γ	peak-enhancement factor for JONSWAP spectrum or Weibull location parameter
γ_{soil}	total unit weight of soil
γ_{soil}'	submerged unit weight of soil
γ_{water}	unit weight of water
γ_s	safety factor on stress amplitude
γ_f	safety factor on natural frequency
γ_{CF}	safety factor for cross-flow screening criterion
γ_{IL}	safety factor for in-line screening criterion
γ_k	safety factor on stability parameter
$\gamma_{on,IL}$	safety factor on onset value for in-line V_R
$\gamma_{on,CF}$	safety factor on onset value for cross-flow V_R
κ_{RFC}	rain flow counting factor
κ	curvature
λ_1	mode shape factor
λ_{max}	equivalent stress factor
η	usage factor
μ	mean value
μ_a	axial friction coefficient
μ_L	lateral friction coefficient
ν	Poisson's ratio or kinematic viscosity ($\approx 1.5 \cdot 10^{-6}$ [m^2/s]
ϕ	mode shape
$\Phi()$	cumulative normal distribution function
$\varphi()$	normal distribution function
φ_s	angle of friction, cohesionless soils
ψ_k^{CM}	correction factor for C_M due to pipe roughness
ψ_{trench}^{CM}	correction factor for C_M due to effect of pipe in trench
ψ_{proxi}^{CM}	reduction factor for C_M due to seabed proximity
$\psi_{KC\alpha}^{CD}$	correction factor for C_D due to Keulean-Carpenter number and current flow ratio.
ψ_{trench}^{CD}	correction factor for C_D due to effect of pipe in trench
ψ_{VIV}^{CD}	amplification factor for C_D due to cross-flow vibrations
ψ_{proxy}^{CD}	reduction factor for C_D due to seabed proximity
$\psi_{proxy,\,onset}$	correction factor for onset cross-flow due to seabed proximity
$\psi_{trench,\,onset}$	reduction factor for onset cross-flow due to the effect of a trench
$\psi_{\alpha,\,IL}$	correction factor for onset of in-line due wave
ρ	density of water
ρ_s/ρ	specific mass ratio between the pipe mass (not including added mass) and the displaced water.
σ	stress, spectral width parameter or standard deviation
σ_c	standard deviation of current velocity fluctuations
σ_u	standard deviation of wave-induced flow velocity
σ_E	environmental stress
σ_{FM}	environmental stress due to direct wave loading
σ_s	effective soil stress or standard deviation of wave-induced stress amplitude
$\sigma_{s,I}$	standard deviation of wave-induced stress amplitude with no drag effect
θ_{rel}	relative angle between flow and pipeline direction
$\bar{\theta}$	flow direction
ζ_T	total modal damping ratio
ζ_{soil}	soil modal damping ratio
ζ_{str}	structural modal damping ratio
ζ_h	hydrodynamic modal damping ratio
ω_n	angular natural frequency
ω	angular wave frequency
ω_p	angular spectral peak wave frequency

1.14.3 Subscripts

IL	in-line
CF	cross-flow
i	cross-flow modes denoted with the index 'i'
j	in-line modes denoted with the index 'j'
onset	onset of VIV
100year	100 year return period value
1year	1 year return period value

2. Design Criteria

2.1 General

2.1.1 For all temporary and permanent free spans a free span assessment addressing the integrity with respect to fatigue (FLS) and local buckling (ULS) shall be performed.

2.1.2 Vibrations due to vortex shedding and direct wave loads are acceptable provided the fatigue and ULS criteria specified herein are fulfilled.

2.1.3 In case several potential vibration modes can become active at a given flow velocity, all these modes shall be considered. Unless otherwise documented the damage contribution for every mode should relate to the same critical (weld) location.

2.1.4 Figure 2-1 shows part of a flow chart for a typical pipeline design. After deciding on diameter, material, wall thickness, trenching or not and coating for weight and insulation, any global buckling design and release of effective axial force needs to be addressed before the free spans are to be assessed. It must be emphasised that the free span assessment must be based on a realistic estimate of the effective axial force, and any changes due to sagging in spans, lateral buckling, end expansion, changes in operational conditions, etc. must be properly accounted for.

Note that sequence in Figure 2-1 is not followed in all projects. Normally an initial routing will be performed before detailed pipeline design is started. As such a typical design process will be to follow this flow chart in iterations until a final, acceptable design is found.

As span length/height and effective axial force may change significantly for different operational conditions, one particular challenge, especially for flow lines, becomes to decide the most critical/governing span scenarios. This will also depend on any global buckling or other release of effective axial force by end expansion or sagging into spans, etc.

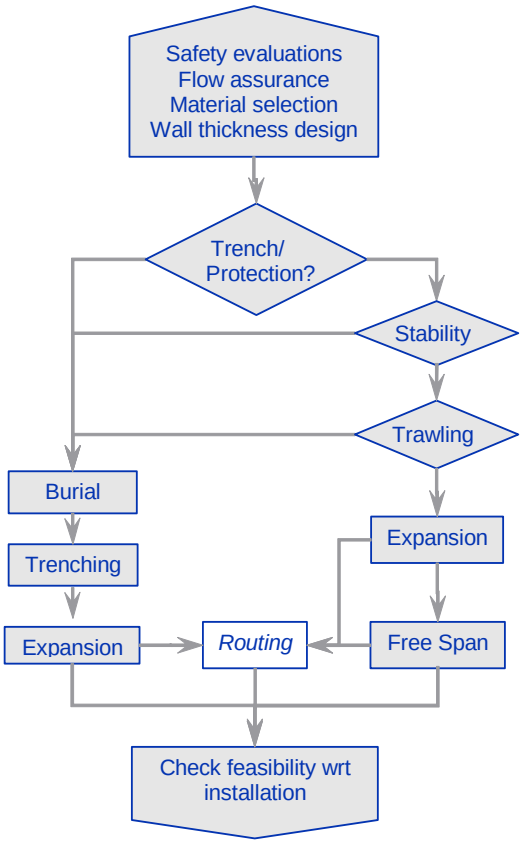

Figure 2-1
Flow chart for pipeline design and free span design

2.1.5 The following functional requirements apply:

- The aim of fatigue design is to ensure an adequate safety against fatigue failure within the design life of the pipeline.
- The fatigue analysis should cover a period which is representative for the free span exposure period.
- All stress fluctuations imposed during the entire design life of the pipeline capable of causing fatigue damage shall be accounted for.
- The local fatigue design checks are to be performed at all free spanning pipe sections accounting for damage contributions from all potential vibration modes related to the considered spans.

2.1.6 Figure 2-2 gives an overview of the required design checks for a free span.

2.2 Non-stationarity of spans

2.2.1 Free spans can be divided into the following main categories:

- Scour induced free spans caused by seabed erosion or bedform activities. The free span scenarios (span length, gap ratio, etc.) may change with time.
- Unevenness induced free spans caused by an irregular seabed profile. Normally the free span scenario is time invariant unless operational parameters such as pressure and temperature change significantly.

2.2.2 In the case of scour induced spans, where no detailed information is available on the maximum expected span length, gap ratio and exposure time, the following apply:

- Where uniform conditions exist and no large-scale mobile bed-forms are present the maximum span length may be taken as the length resulting in a static mid span deflection equal to one external diameter (including any coating).
- The exposure time may be taken as the remaining operational lifetime or the time duration until possible intervention works will take place. All previous damage accumulation must be included.

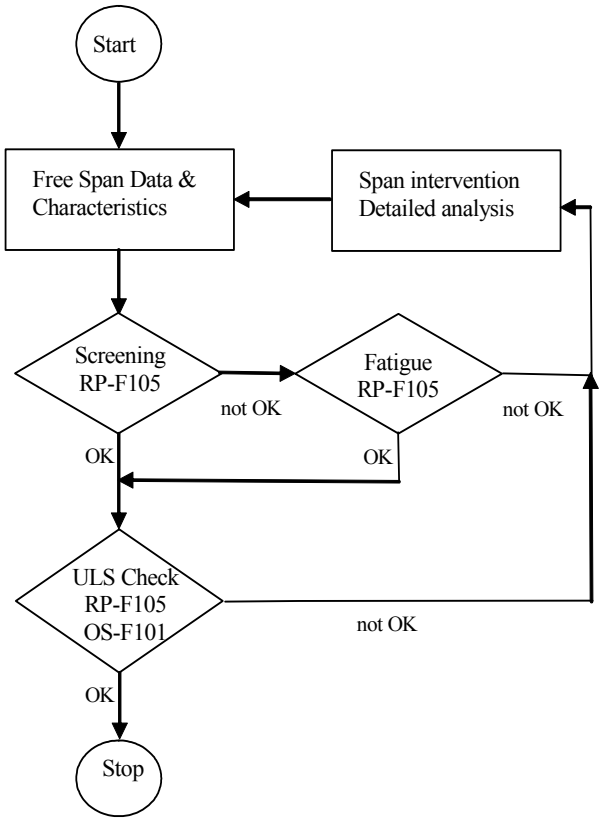

Figure 2-2
Flow chart over design checks for a free span

2.2.3 Additional information (e.g. free span length, gap ratio, natural frequencies) from surveys combined with an inspection strategy may be used to qualify scour induced free spans. These aspects are not covered in this document. Guidance may be found in Mørk et al. (1999) and Fyrileiv et al. (2000).

2.2.4 Changes in operational conditions such as pressure and temperature may cause significant changes in span characteristics and must be accounted for in the free span assessment.

Guidance note:

One example may be flowlines installed on uneven seabed and which buckle during operation. The combination of shut-down and lateral buckles may cause tension in the pipeline and several free spans to develop.

The span length and span height may vary significantly over the range of operational conditions (pressure/temperature). In such cases the whole range of operational conditions should be checked as the lowest combination may be governing for the free span design.

---e-n-d---of---G-u-i-d-a-n-c-e---n-o-t-e---

2.2.5 Other changes during the design life such as corrosion must also be considered in the span assessment where relevant.

Guidance note:

Subtracting half the corrosion allowance when performing the span assessment may be applied in case of no better information.

---e-n-d---of---G-u-i-d-a-n-c-e---n-o-t-e---

2.3 Screening fatigue criteria

2.3.1 The screening criteria proposed herein apply to fatigue caused by Vortex Induced Vibrations (VIV) and direct wave loading in combined current and wave loading conditions. The screening criteria have been calibrated against full fatigue analyses to provide a fatigue life in excess of 50 years. The criteria apply to spans with a response dominated by the 1st symmetric mode (one half wave) and should preferably be applied for screening analyses only. If violated, more detailed fatigue analyses should be performed. The ULS criterion in 2.5 must always be checked.

Guidance note:

The screening criteria as given in 2.3 are calibrated with safety factors to provide a fatigue life in excess of 50 years. As such these criteria are intended to be used for the operational phase.

However, by applying the 10 year return period value for current for the appropriate season, $U_{c,10year}$, instead of the 100 year return period value, the criteria may be used also for the temporary phases (as-laid/empty and flooded).

---e-n-d---of---G-u-i-d-a-n-c-e---n-o-t-e---

2.3.2 The screening criteria proposed herein are based on the assumption that the current velocity may be represented by a 3-parameter Weibull distribution. If this is not the case, e.g. for bi-modal current distributions, care must be taken and the applicability of these screening criteria checked by full fatigue calculations.

2.3.3 The in-line natural frequencies $f_{n,IL}$ must fulfil:

$$\frac{f_{n,IL}}{\gamma_{IL}} > \frac{U_{c,100\,year}}{V_{R,onset}^{IL} \cdot D} \cdot \left(1 - \frac{L/D}{250}\right) \cdot \frac{1}{\bar{\alpha}}$$

where

γ_{IL} Screening factor for in-line, see 2.6

$\bar{\alpha}$ $\text{Current flow ratio} = \dfrac{U_{c,100\,year}}{U_{w,1year} + U_{c,100\,year}}$

Minimum value of 0.6.

D Outer pipe diameter incl. coating

L Free span length

$U_{c,100year}$ 100 year return period value for the current velocity at the pipe level, see Sec.3

$U_{w,1year}$ Significant 1 year return period value for the wave-induced flow velocity at the pipe level corresponding to the annual significant wave height $H_{s,1year}$, see Sec.3

$V_{R,onset}^{IL}$ In-line onset value for the reduced velocity, see Sec.4.

If the above criterion is violated, then a full in-line VIV fatigue analysis is required.

2.3.4 The cross-flow natural frequencies $f_{n,CF}$ must fulfil:

$$\frac{f_{n,CF}}{\gamma_{CF}} > \frac{U_{c,100\,year} + U_{w,1\,year}}{V_{R,onset}^{CF} \cdot D}$$

where

γ_{CF} Screening factor for cross-flow, see 2.6

$V_{R,onset}^{CF}$ Cross-flow onset value for the reduced velocity, see Sec.4

If the above criterion is violated, then a full in-line and cross-flow VIV fatigue analysis is required.

2.3.5 If a fatigue analysis is required, a simplified estimate of the fatigue damage can be computed by adding the wave induced flow to the current long-term distribution or neglecting the influence of the waves for deepwater pipelines. If this criterion is violated, then a full fatigue analyses due direct wave action is required.

2.3.6 Fatigue analysis due to direct wave action is not required provided:

$$\frac{U_{c,100\,year}}{U_{w,1year} + U_{c,100\,year}} > \frac{2}{3}$$

and the above screening criteria for in-line VIV are fulfilled. If this criterion is violated, then a full fatigue analyses due to in-line VIV and direct wave action is required.

Guidance note:

Section 2.3.6 states that full fatigue analysis is required if the 1-year significant wave-induced flow at pipe level is larger than half the 100-year current velocity at pipe level.

It is also possible to apply the screening criteria in the same way as the traditional on-set criterion in order to establish conservative allowable free span lengths even though the above mentioned wave effect criterion is violated.

If the flow is current dominated, the free span may be assessed by adding a characteristic wave-induced flow component to the current velocity as expressed in the in-line VIV screening criterion, i.e. 1-year return period wave induced flow.

If the flow velocity is dominated by the waves, then generally a full fatigue analysis has to be performed. However, the in-line VIV screening criterion may still be used provided that a quasi-static Morison force calculation shows that the fatigue due to direct wave action could be neglected or is insignificant compared to in-line VIV fatigue.

---e-n-d---of---G-u-i-d-a-n-c-e---n-o-t-e---

2.4 Fatigue criterion

2.4.1 The fatigue criterion can be formulated as:

$$\eta \cdot T_{life} \geq T_{exposure}$$

where η is the allowable fatigue damage ratio, T_{life} the fatigue design life capacity and $T_{exposure}$ the design life or load exposure time.

2.4.2 The fatigue damage assessment is based on the accumulation law by Palmgren-Miner:

$$D_{fat} = \sum \frac{n_i}{N_i}$$

where

D_{fat} Accumulated fatigue damage.

n_i Total number of stress cycles corresponding to the (mid-wall) stress range S_i

N Number of cycles to failure at stress range S_i

Σ Implies summation over all stress fluctuations in the design life

2.4.3 The number of cycles to failure at stress range S is defined by the SN curve of the form:

$$N = \begin{cases} \bar{a}_1 \cdot S^{-m_1} & S > S_{sw} \\ \bar{a}_2 \cdot S^{-m_2} & S \leq S_{sw} \end{cases}$$

where

m_1, m_2 Fatigue exponents (the inverse slope of the bi-linear S-N curve)

$\bar{a}_1, \bar{a}_2$ Characteristic fatigue strength constant defined as the mean-minus-two-standard-deviation curve

S_{sw} Stress at intersection of the two SN-curves given by:

$$S_{sw} = 10^{\left(\frac{\log \bar{a}_1 - \log N_{sw}}{m_1}\right)}$$

where N_{sw} is the number of cycles for which change in slope appear. Log N_{sw} is typically 6 – 7.

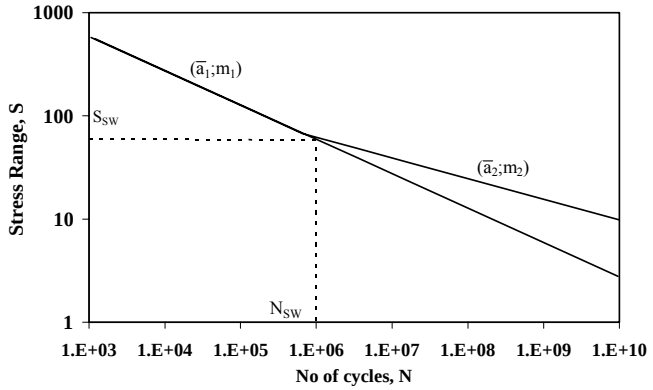

Figure 2-3
Typical two-slope SN curve

2.4.4 The SN-curves may be determined from:

— dedicated laboratory test data
— accepted fracture mechanics theory, or
— DNV-RP-C203 "Fatigue Strength Analysis of Offshore Steel Structures".

The SN-curve must be applicable for the material, construction detail, location of the initial defect (crack initiation point) and corrosive environment. The basic principles in DNV-RP-C203 apply.

Guidance note:

Crack growth analyses may be used as an alternative to fatigue assessment using Miner Palmgren summation and SN-curves provided that an accepted fracture mechanics theory is applied, using a long-term distribution of stress ranges calculated by this document and that the safety against fatigue failure is accounted for and documented in a proper manner.

---e-n-d---of---G-u-i-d-a-n-c-e---n-o-t-e---

2.4.5 The fatigue life capacity, T_{life}, can be formally expressed as:

$$T_{life} = \frac{1}{\sum\left(\frac{f_v \cdot S_i^m \cdot P_i}{\bar{a}}\right)}$$

where

P_i Probability of occurrence for the "i"th stress cycle
f_v Vibration frequency

2.4.6 The concept adopted for the fatigue analysis applies to both response models and force models. The stress ranges to be used may be determined by:

— a response model, see Sec.4
— a force model, see Sec.5.

2.4.7 The following approach is recommended:

— The fatigue damage is evaluated independently in each sea-state, i.e., the fatigue damage in each cell of a scatter diagram in terms of (H_s, T_p, θ) times the probability of occurrence for the individual sea state.
— In each sea-state (H_s, T_p, θ) is transformed into (U_w, T_u) at the pipe level as described in Sec.3.3.
— The sea state is represented by a significant short-term flow induced velocity amplitude U_w with mean zero up-crossing period T_u, i.e. by a train of regular wave-induced flow velocities with amplitude equal to U_w and period T_u. The effect of irregularity will reduce the number of large amplitudes. Irregularity may be accounted for provided it is properly documented.
— Integration over the long-term current velocity distribution for the combined wave and current flow is performed in each sea-state.

2.4.8 The total fatigue life capacities in the in-line and cross-flow directions are established by integrating over all sea-states, i.e.

$$T_{life}^{IL} = \left(\sum_{\theta}\sum_{H_S}\sum_{T_P} \frac{P_{Hs,Tp,\theta}}{\min\left(T_{Hs,Tp,\theta}^{RM,IL}, T_{Hs,Tp,\theta}^{FM,IL}\right)}\right)^{-1}$$

$$T_{life}^{CF} = \left(\sum_{\theta}\sum_{H_S}\sum_{T_P} \frac{P_{Hs,Tp,\theta}}{T_{Hs,Tp,\theta}^{RM,CF}}\right)^{-1}$$

Where $P_{H_s,T_p,\theta}$ is the probability of occurrence of each individual sea-state, i.e. the probability of occurrence reflected by the cell in a scatter diagram. The in-line fatigue life capacity is conservatively taken as the minimum capacity (i.e., maximum damage) from VIV (RM) or direct wave loads (FM) in each sea state.

The fatigue life is the minimum of the in-line and the cross-flow fatigue lives.

2.4.9 The following marginal fatigue life capacities are evaluated for (all) sea states characterised by (H_s, T_p, θ).

$T_{Hs,Tp,\theta}^{RM,IL}$	Marginal fatigue capacity against in-line VIV and cross-flow induced in-line motion in a single sea-state (H_s, T_p, θ) integrated over long term pdf for the current, see Sec.4.2.2.
$T_{Hs,Tp,\theta}^{RM,CF}$	Marginal fatigue capacity against cross-flow VIV in a sea-state (H_s, T_p, θ) integrated over long term pdf for the current, see Sec.4.2.1.
$T_{Hs,Tp,\theta}^{FM,IL}$	Marginal fatigue capacity against direct wave actions in a single sea-state characterised by (H_s, T_p, θ) using mean value of current, see Sec.5.2.2.

2.4.10 Unless otherwise documented, the following assumptions apply:

— The current and wave-induced flow components at the pipe level are statistically independent.
— The current and wave-induced flow components are assumed co-linear. This implies that the directional probability of occurrence data for either waves or current (the most conservative with respect to fatigue damage) must be used for both waves and current.

2.5 ULS criterion

2.5.1 Local buckling check for a pipeline free span shall be in compliance with the combined loading – load controlled condition criteria in DNV-OS-F101, Sec.5 or similar stress-based criteria in a recognised code. Functional and environmental bending moment, axial force and pressure shall be accounted for. Simplifications are allowed provided verification is performed by more advanced modelling/analyses in cases where the ULS criteria become governing.

2.5.2 Typically the load effects to be considered in the ULS checks shall be:

Vertical direction:

— static bending (self weight, seabed profile, etc.)
— cross-flow VIV
— trawl gear interaction.

Horizontal direction:

— in-line VIV
— direct drag and inertia load effects from combined wave and current
— trawl gear interaction.

Note that different soil stiffnesses should be used for different load directions and load rates (static/dynamic).

2.5.3 For the operating condition the environmental bending moment shall be taken as the most probable 100-year return period value (10^{-2} annual exceedence probability). For temporary conditions the return period value depends on the seasonal timing and duration of the temporary period.

2.5.4 If more information is not available the following return period values may be applied:

— A 100 year return period if the duration exceeds 6 months.
— A 10 year return period for the actual seasonal environmental condition if the duration exceeds 3 days but is less than 6 months.
— For temporary conditions with duration less than 3 days or operations which can be terminated within a 3 days window, environmental data may be based on reliable weather forecasts.

2.5.5 Environmental events with a given return period require information on joint wave and on-bottom current (and directionality) probabilities. If more detailed information is not available the following cases may be applied (assuming co-linear wave and current flow).

	(H_s, T_p)	U_c
Case 1:	100 year	1 year
Case 2:	1 year	100 year

2.5.6 For extreme wave conditions, which can be assumed to cause large deformations on the span shoulders, detailed analyses of the soil stiffness at the shoulders may be required. In lieu of detailed documentation, the boundary conditions for the free span should be assumed as pinned-pinned (for direct wave load cases).

2.5.7 The maximum environmental bending moment due to in-line and cross-flow VIV or direct wave and current action may be found from the dynamic stresses:

$$M_E = \sigma_E \frac{2 \cdot I}{D_s - t}$$

where

σ_E Maximum environmental stress given below
I Moment of inertia
D_s Outer diameter of steel pipe
T Wall thickness

2.5.8 The maximum environmental stress, σ_E, is taken as:

$$in-line \qquad \sigma_E = \frac{1}{2}\max\left\{S_{IL}\ ;\ 0.4 \cdot S_{CF}\ \frac{A_{IL}}{A_{CF}}\right\} + \sigma_{FM,\max}$$

$$cross-flow \quad \sigma_E = \frac{1}{2} S_{CF}$$

where

S_{IL} In-line stress range, see Sec.4.3
S_{CF} Cross-flow stress range, see Sec.4.4
$\sigma_{FM,max}$ Maximum environmental stress due to direct wave loading, see below
A_{IL} In-line unit deflection stress amplitude due to VIV, see Sec.4.3
A_{CF} Cross-flow unit deflection stress amplitude due to VIV, see Sec.4.4

For the cross-flow direction, the stress simply stems from the VIV induced amplitude. For the in-line direction, the dynamic stress range is taken as the maximum of:

— the return period stress range for in-line VIV, S_{IL}, defined in 4.3
— the stress from 40% of the CF induced VIV motion. All parameters are defined in Sec.4.4.

2.5.9 Two different methods can be applied to establish the maximum environmental stress, $\sigma_{FM,max}$ (see DNV-OS-F201 for more information):

— design based on response statistics
— design based on environmental statistics.

For free span analysis design based on environmental statistics is considered appropriate using:

— a Design Storm approach with irregular wave analysis in time domain (TD) or irregular wave analyses in frequency domain (FD), or
— a Design Wave approach using regular wave analysis in TD, i.e., with bending moment calculated from H_{max}.

2.5.10 The Design Wave approach may use a set of appropriate design cases (in terms of wave height, wave period, current and directionality) likely to produce the extreme response with a chosen return period. This may be done using a return period value for H_s with a wave period variation covering a realistic variation range (e.g. 90% confidence interval) or using environmental contours.

Guidance note:

Cases with moderate H_s and large wave period are often governing. Hence more focus should be given to large T_p values.

In case of a quasi-static and not dynamically sensitive pipeline response for the ULS condition, the 100-year H_{max} value with an associated period could be used to generate the regular wave and corresponding quasi-static response.

---e-n-d---of---G-u-i-d-a-n-c-e---n-o-t-e---

2.5.11 The maximum environmental stress, $\sigma_{FM,max}$, from direct wave loading can be established using a time domain Design Storm approach as follows:

1) Global time domain response analysis is performed for the actual stationary environmental condition. A typical storm duration may be taken as 3 hours.
2) Time histories for the dynamic stress are established
3) A 3-parameter Weibull distribution is fitted to the individual stress maxima between successive mean value crossings $\sigma_{FM}(t)$.

4) A Gumbel distribution is established for the extreme value for the largest individual maxima of $\sigma_{FM}(t)$ for the 3 hour duration.

5) $\sigma_{FM,max}$ is estimated as the p-percentile in the Gumbel distribution, i.e., the 57% percentile for the expected value or the Most Probable Maximum value corresponding to a 37% percentile

2.5.12 As a simplified alternative $\sigma_{FM,max}$ may be calculated using:

$$\sigma_{FM,max} = k_p \cdot k_M \cdot \sigma_s$$
$$k_p = \sqrt{2\ln(f_v \Delta T)}$$
$$k_M = 1 + \frac{1}{2}\left[\frac{\sigma_s}{\sigma_{s,I}} - 1\right]$$

where k_p is a peak factor where ΔT is the storm duration equal to 3 hour and f_v is the vibration frequency. σ_s is the standard deviation of the stress response $\sigma_{FM}(t)$ and $\sigma_{s,I}$ is the standard deviation for the stress response without drag loading. σ_s and $\sigma_{s,I}$ may be calculated from a time domain or frequency domain analysis, see Sec.5. k_M is a factor accounting for non-linearity in the drag loading. A static stress component may be added if relevant.

Guidance note:

In case the ULS due to direct wave action is found to be governing, the effect of the axial force should be considered.

---e-n-d---of---G-u-i-d-a-n-c-e---n-o-t-e---

2.5.13 For temporary conditions extreme environmental conditions, like a 10-year flow velocity sustained for a given time period, may cause fatigue damage to develop. To ensure the integrity of the pipeline and the robustness of the design, such extreme events should be checked.

2.6 Safety factors

2.6.1 The safety factors to be used with the screening criteria are listed below.

Table 2-1 Safety factors for screening criteria	
γ_{IL}	1.4
γ_{CF}	1.4

2.6.2 Pipeline reliability against fatigue uses the safety class concept, which takes account of the failure consequences, see DNV-OS-F101, Sec.2.

The following safety factor format is used:

$$D_{fat,RP-F105} = T_{exposure} \cdot \sum \frac{f_v\left(\gamma_s S(\gamma_f, \gamma_k, \gamma_{on}.)\right)^m P(\bullet)}{\bar{a}} \leq \eta$$

γ_f, γ_{on}, γ_k and γ_s denote partial safety factors for the natural frequency, onset of VIV, stability parameter and stress range respectively. The set of partial safety factor to be applied for both response models and force models are specified in the tables below for the individual safety classes.

Table 2-2 General safety factors for fatigue			
Safety factor	*Safety Class*		
	Low	*Normal*	*High*
η	1.0	0.5	0.25
γ_k	1.0	1.15	1.30
γ_s	1.3		
$\gamma_{on,\ IL}$	1.1		
$\gamma_{on,\ CF}$	1.2		

Table 2-3 Safety factor for natural frequencies, γ_f			
Free span type	*Safety Class*		
	Low	*Normal*	*High*
Very well def.	1.0	1.0	1.0
Well def.	1.05	1.1	1.15
Not well def.	1.1	1.2	1.3

Comments:

— γ_s is to be multiplied to the stress range ($S\ \gamma_S$)
— γ_f applies to the natural frequency (f_n/γ_f)
— γ_{on} applies to onset values for in-line and cross-flow VIV ($V_{R,on}^{CF} / \gamma_{on,CF}$ and $V_{R,on}^{IL} / \gamma_{on,IL}$)
— γ_k applies to the total damping
— for ULS, the calculation of load effects is to be performed without safety factors ($\gamma_S = \gamma_f = \gamma_k = \gamma_{on} = 1.0$), see also 2.6.5.

2.6.3 The free spans shall be categorised as:

Not well defined – spans where important span characteristics like span length, gap and effective axial force are not accurately determined/measured.

Selection criteria for this category are (but not limited to):

— erodible seabed (scouring)
— environmental conditions given by extreme values only
— operational conditions change the span scenario and these changes are not assessed in detail, or
— span assessment in an early stage of a project development.

Well defined – spans where important span characteristics like span length, gap and effective axial force are determined/measured. Site specific soil conditions and a long-term description of the environmental conditions exist.

Very well defined – spans where important span characteristics like span length, gap and effective axial force are determined/measured with a high degree of accuracy. The soil conditions and the environmental conditions along the route are well known.

Requirements:

— span length/gap actually measured and well defined due to span supports or uneven seabed
— structural response quantities by FE analysis
— soil properties by soil samples along route
— site specific long-term distributions of environmental data
— effect of changes in operational conditions evaluated in detail.

2.6.4 In case several phases with different safety classes are to be accounted for, the highest safety class is to be applied for all phases as fatigue damage accumulates.

2.6.5 The reliability of the pipeline against local buckling (ULS criterion) is ensured by use of the safety class concept as implemented by use of safety factors according to DNV-OS-F101, Sec.5 D500 or Sec.12.

2.6.6 The relationship between the fatigue life, exposure time and fatigue damage is:

$$D_{fat,RP-F105} = \frac{T_{exposure}}{T_{life}} \cdot \eta$$

2.6.7 As stated in DNV-OS-F101 Sec.5 D703, all stress fluctuations imposed to the pipeline including the construction/installation phase shall be accounted for when calculating the

fatigue damage. This means that the total accumulated fatigue damage from different sources shall not exceed the allowable damage ratios of DNV-OS-F101. As the allowable damage ratio of DNV-OS-F101 is different from the one in Table 2-2 due to use of partial safety factors in RP-F105, the calculated damage ratio according to RP-F105 may be converted into a corresponding DNV-OS-F101 damage ratio by the following relation:

$$D_{fat,OS-F101} = \frac{D_{fat,RP-F105}}{\eta} \cdot \alpha_{fat}$$

Where the α_{fat} denotes the allowable damage ratio according to DNV-OS-F101.

3. Environmental Conditions

3.1 General

3.1.1 The objective of the present section is to provide guidance on:

— the long term current velocity distribution
— short-term and long-term description of wave-induced flow velocity amplitude and period of oscillating flow at the pipe level
— return period values.

3.1.2 The environmental data to be used in the assessment of the long-term distributions shall be representative for the particular geographical location of the pipeline free span.

3.1.3 The flow conditions due to current and wave action at the pipe level govern the response of free spanning pipelines.

3.1.4 The environmental data must be collected from periods that are representative for the long-term variation of the wave and current climate. In case of less reliable or limited wave and current data, the statistical uncertainty should be assessed and, if significant, included in the analysis.

3.1.5 Preferably, the environmental load conditions should be established near the pipeline using measurement data of acceptable quality and duration. The wave and current characteristics must be transferred (extrapolated) to the free span level and location using appropriate conservative assumptions.

3.1.6 The following environmental description may be applied:

— directional information, i.e., flow characteristic versus sector probability, or
— omnidirectional statistics may be used if the flow is uniformly distributed.

If no such information is available, the flow should be assumed to act perpendicular to the axis of the pipeline at all times.

3.2 Current conditions

3.2.1 The steady current flow at the free span level may have components from:

— tidal current
— wind induced current
— storm surge induced current
— density driven current.

Guidance note:

The effect of internal waves, which are often observed in parts of South East Asia, need to be taken into account for the free span assessment. The internal waves may have high fluid particle velocity and they can be modelled as equivalent current distributions.

---e-n-d---of---G-u-i-d-a-n-c-e---n-o-t-e---

3.2.2 For water depths greater than 100 m, the ocean currents can be characterised in terms of the driving and steering agents:

— The driving agents are tidal forces, pressure gradients due to surface elevation or density changes, wind and storm surge forces.
— The steering agents are topography and the rotation of the earth.

The modelling should account adequately for all agents.

3.2.3 The flow can be divided into two zones:

— An **Outer Zone** far from the seabed where the mean current velocity and turbulence vary only slightly in the horizontal direction.
— An **Inner Zone** where the mean current velocity and turbulence show significant variations in the horizontal direction and the current speed and direction is a function of the local sea bed geometry.

3.2.4 The outer zone is located approximately one local seabed form height above the seabed crest. In case of a flat seabed, the outer zone is located approximately at height (3600 z_0) where z_0 is the bottom roughness, see Table 3-1.

3.2.5 Current measurements using a current meter should be made in the outer zone outside the boundary layer at a level 1-2 seabed form heights above the crest. For large-scale currents, such as wind driven and tidal currents, the choice of measurement positions may be based on the variations in the bottom topography assuming that the current is geo-strophic, i.e., mainly running parallel to the large-scale bottom contours.

Over smooth hills, flow separation occurs when the hill slope exceeds about 20^o. Current data from measurements in the boundary layer over irregular bed forms are of little practical value when extrapolating current values to other locations.

3.2.6 In the inner zone the current velocity profile is approximately logarithmic in areas where flow separation does not occur:

$$U(z) = R_c \cdot U(z_r) \frac{(\ln(z) - \ln(z_0))}{(\ln(z_r) - \ln(z_0))}$$

where

R_c reduction factor, see Sec.3.4.1.
z elevation above the seabed
z_r reference measurement height (in the outer zone)
z_0 bottom roughness parameter to be taken from Table 3-1.

Table 3-1 Seabed roughness

Seabed	*Roughness z_0 (m)*
Silt	$\approx 5 \cdot 10^{-6}$
fine sand	$\approx 1 \cdot 10^{-5}$
Medium sand	$\approx 4 \cdot 10^{-5}$
coarse sand	$\approx 1 \cdot 10^{-4}$
Gravel	$\approx 3 \cdot 10^{-4}$
Pebble	$\approx 2 \cdot 10^{-3}$
Cobble	$\approx 1 \cdot 10^{-2}$
Boulder	$\approx 4 \cdot 10^{-2}$

3.2.7 If no detailed analyses are performed, the mean current values at the free span location may assume the values at the nearest suitable measurement point. The flow (and macro-roughness) is normally 3D and transformation of current characteristics should account for the local bottom topography e.g. be guided by numerical simulations.

3.2.8 For conditions where the mean current is spread over a small sector (e.g. tide-dominated current) and the flow condition can be assumed to be bi-directional, the following model may be applied in transforming the mean current locally. It is assumed that the current velocity $U(z_r)$ in the outer zone is known, see Figure 3-1. The velocity profile $U(z^*)$ at a location near the measuring point (with $z_r^* > z_r$) may be approximated by:

$$U(z^*) = U(z_r)\frac{\left(\ln(z^*) - \ln(z_m)\right)}{\left(\ln(z_r^*) - \ln(z_m)\right)}$$

The "macro-roughness" parameter z_m is given by:

$$\ln(z_m) = \ln(z_r^*) - \frac{z_r^*}{\left(z_r^* - z_r\right) + \frac{z_r}{\left(\ln(z_r) - \ln(z_o)\right)}}$$

z_m is to be taken less than 0.2.

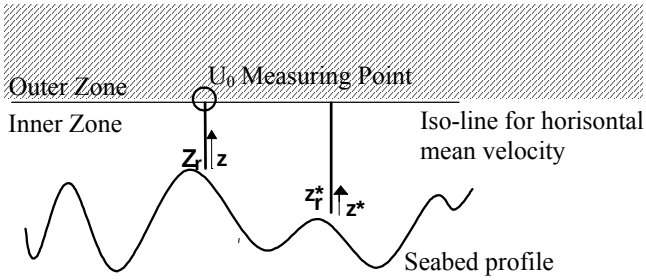

Figure 3-1
Definitions for 2D model

3.2.9 It is recommended to perform current measurements with 10 min or 30 min averages for use with FLS.

3.2.10 For ULS, 1 min average values should be applied. The 1 minute average values may be established from 10 or 30 min average values as follows:

$$U_{1\min} = \begin{cases} (1 + 1.9 \cdot I_c) \cdot U_{10\min} \\ (1 + 2.3 \cdot I_c) \cdot U_{30\min} \end{cases}$$

where I_c is the turbulence intensity defined below.

3.2.11 The turbulence intensity, I_c, is defined by:

$$I_c = \frac{\sigma_c}{U_c}$$

where σ_c is the standard deviation of the velocity fluctuations and U_c is the 10 min or 30 min average (mean) velocity (1 Hz sampling rate).

3.2.12 If no other information is available, the turbulence intensity should be taken as 5%. Experience indicates that the turbulence intensity for macro-roughness areas is 20-40% higher than the intensity over a flat seabed with the same small-scale seabed roughness. The turbulence intensities in a rough seabed area to be applied for in-line fatigue assessment may conservatively be taken as typical turbulence intensities over a flat bottom (at the same height) with similar small-scale seabed roughness.

3.2.13 Detailed turbulence measurements, if deemed essential, should be made at 1 m and 3 m above the seabed. High frequency turbulence (with periods lower than 1 minute) and low frequency turbulence must be distinguished.

3.2.14 The current speed in the vicinity of a platform may be reduced from the specified free stream velocity, due to hydrodynamic shielding effects. In absence of a detailed evaluation, the guidance on blockage factors given in ISO 13819-2, ISO 19902 to ISO 19906 can be used.

3.2.15 Possible changes in the added mass (and inertia actions) for closely spaced pipelines and pipeline bundles should also be accounted for.

3.3 Short-term wave conditions

3.3.1 The wave-induced oscillatory flow condition at the free span level may be calculated using numerical or analytical wave theories. The wave theory shall be capable of describing the conditions at the pipe location, including effects due to shallow water, if applicable. For most practical cases, linear wave theory can be applied. Wave boundary layer effects can normally be neglected.

3.3.2 The short-term, stationary, irregular sea states may be described by a wave spectrum $S_{\eta\eta}(\omega)$ i.e. the power spectral density function of the sea surface elevation. Wave spectra may be given in table form, as measured spectra, or in an analytical form.

3.3.3 The JONSWAP or the Pierson-Moskowitz spectra are often appropriate. The spectral density function is:

$$S_{\eta\eta}(\omega) = \alpha g^2 \omega^{-5} \exp\left(-\frac{5}{4}\left(\frac{\omega}{\omega_p}\right)^{-4}\right) \gamma^{\exp\left(-0.5\left(\frac{\omega-\omega_p}{\sigma\ \omega_p}\right)^2\right)}$$

where

ω = $2\pi/T_w$ is the angular wave frequency.
T_w Wave period.
T_p Peak period.
ω_p = $2\pi/T_p$ is the angular spectral peak frequency
g Gravitational acceleration.

The Generalised Phillips' constant is given by:

$$\alpha = \frac{5}{16} \cdot \frac{H_s^{\ 2} \omega_p^{\ 4}}{g^2} \cdot (1 - 0.287 \ln \gamma)$$

The spectral width parameter is given by:

$$\sigma = \begin{cases} 0.07 & if \ \ \omega \le \omega_p \\ 0.09 & else \end{cases}$$

The peak-enhancement factor is given by:

$$\gamma = \begin{cases} 5 & \varphi \le 3.6 \\ \exp(5.75 - 1.15\varphi) & 3.6 < \varphi < 5 \\ 1 & \varphi \ge 5 \end{cases} \quad ; \quad \varphi = \frac{T_p}{\sqrt{H_S}}$$

where H_s is to be given in metres and T_p in seconds.

The Pierson-Moskowitz spectrum appears for $\gamma = 1.0$.

3.3.4 Both spectra describe wind sea conditions that are reasonable for the most severe seastates. However, moderate and low sea states, not dominated by limited fetch, are often composed of both wind-sea and swell. A two peak (bi-modal) spectrum should be considered to account for swell if considered important.

3.3.5 The wave-induced velocity spectrum at the pipe level $S_{UU}(\omega)$ may be obtained through a spectral transformation of the waves at sea level using a first order wave theory:

$$S_{UU}(\omega) = G^2(\omega) \cdot S_{\eta\eta}(\omega)$$

$G^2(\omega)$ is a frequency transfer function from sea surface elevation to wave-induced flow velocities at pipe level given by:

$$G(\omega) = \frac{\omega \cdot \cosh\left(k \cdot (D+e)\right)}{\sinh\left(k \cdot h\right)}$$

Where h is the water depth and k is the wave number established by iteration from the transcendental equation:

$$kh = \frac{\omega^2 \cdot h}{g} \coth\left(k \cdot h\right)$$

Guidance note:

Note that this transfer function is valid for Airy wave theory only and is strictly speaking not applicable for shallow water.

---e-n-d---of---G-u-i-d-a-n-c-e---n-o-t-e---

3.3.6 The spectral moments of order n is defined as:

$$M_n = \int_0^\infty \omega^n S_{UU}(\omega) d\omega$$

The following spectrally derived parameters appear:

— Significant flow velocity amplitude at pipe level:

$$U_S = 2\sqrt{M_0}$$

— Mean zero up-crossing period of oscillating flow at pipe level:

$$T_u = 2\pi \sqrt{\frac{M_0}{M_2}}$$

U_S and T_u may be taken from Figure 3-2 and Figure 3-3 assuming linear wave theory.

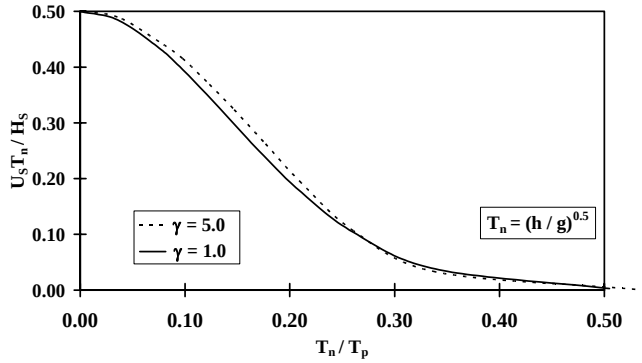

Figure 3-2
Significant flow velocity amplitude at pipe level, U_S

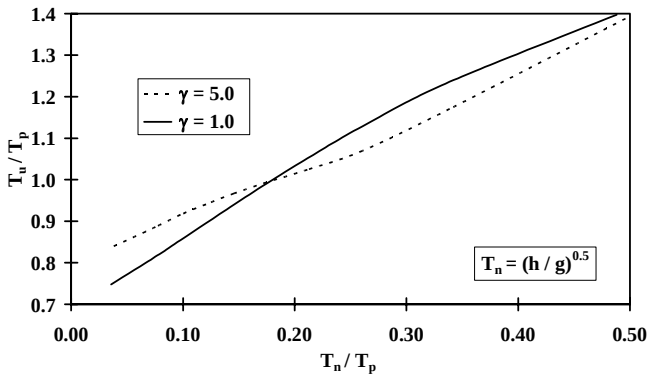

Figure 3-3
Mean zero up-crossing period of oscillating flow at pipe level, T_u

3.4 Reduction functions

3.4.1 The mean current velocity over a pipe diameter (i.e. taken as current at e + D/2) applies. Introducing the effect of directionality, the reduction factor, R_c becomes:

$$R_c = \sin(\theta_{rel})$$

where θ_{rel} is the relative direction between the pipeline direction and the current flow direction.

3.4.2 In case of combined wave and current flow the apparent seabed roughness is increased by the non-linear interaction between wave and current flow. The modified velocity profile and hereby-introduced reduction factor may be taken from DNV-RP-E305.

3.4.3 The effect of wave directionality and wave spreading is introduced in the form of a reduction factor on the significant flow velocity, i.e. projection onto the velocity normal to the pipe and effect of wave spreading.

$$U_W = U_S \cdot R_D$$

The reduction factor is given by, see Figure 3-4.

$$R_D = \sqrt{\int_{-\pi/2}^{\pi/2} w(\beta) \sin^2(\theta_{rel} - \beta) d\beta}$$

where θ_{rel} is the relative direction between the pipeline direction and wave direction

3.4.4 The wave energy spreading (directional) function given by a frequency independent cosine power function is:

$$w(\beta) = \begin{cases} k_w \cos^s(\beta) & |\beta| < \frac{\pi}{2} \\ 0 & else \end{cases} \quad ; \quad k_w = \sqrt{\frac{1}{\pi}} \frac{\Gamma\left(1 + \frac{s}{2}\right)}{\Gamma\left(\frac{1}{2} + \frac{s}{2}\right)}$$

Γ is the gamma function, see 3.5.1, and s is a spreading parameter, typically modelled as a function of the sea state. Normally s is taken as an integer, between 2 and 8, $2 \le s \le 8$. If no information is available, the most conservative value in the range 2-8 shall be selected. For current flow s > 8.0 may be applied.

Guidance note:

Cases with large H_S and large T_p values may have a lower spread. The wave spreading approach, as given in NORSOK N-003, can also be considered as an alternative approach.

---e-n-d---of---G-u-i-d-a-n-c-e---n-o-t-e---

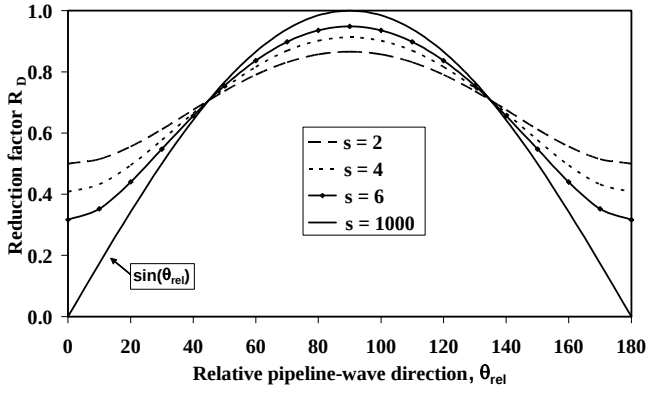

Figure 3-4
Reduction factor due to wave spreading and directionality

3.5 Long-term environmental modelling

3.5.1 A 3-parameter Weibull distribution is often appropriate for modelling of the long-term statistics for the current velocity U_c or significant wave height, H_s. The Weibull distribution is given by:

$$F_X(x) = 1 - \exp\left(-\left(\frac{x-\gamma}{\alpha}\right)^{\beta}\right)$$

where F(•) is the cumulative distribution function and α is the scale, β is the shape and γ is the location parameter. Note that the Rayleigh distribution is obtained for β = 2 and an Exponential distribution for β = 1.

The Weibull distribution parameters are linked to the statistical moments (μ: mean value, σ: standard deviation, δ: skewness) as follows:

$$\mu = \alpha\Gamma\left(1+\frac{1}{\beta}\right)+\gamma$$

$$\sigma = \alpha\sqrt{\Gamma\left(1+\frac{2}{\beta}\right)-\Gamma\left(1+\frac{1}{\beta}\right)^2}$$

$$\delta = \left(\frac{\alpha}{\sigma}\right)^3\cdot\left(\Gamma\left(1+\frac{3}{\beta}\right)-3\Gamma\left(1+\frac{1}{\beta}\right)\Gamma\left(1+\frac{2}{\beta}\right)+2\Gamma\left(1+\frac{1}{\beta}\right)^3\right)$$

Γ is the Gamma function defined as:

$$\Gamma(x) = \int_0^{\infty} t^{x-1}e^{-t}\,dt$$

3.5.2 The directional (i.e. versus θ) or omni-directional current data can be specified as follows:

— A histogram in terms of (U_c, θ) versus probability of occurrence.

The fatigue analysis is based on the discrete events in the histogram. The corresponding Return Period Values (RPV) are estimated from the corresponding exceedance probability in the histogram or from a fitted pdf, see 3.6.

— A long term probability density function (pdf).

The corresponding Return Period Values for 1, 10 and 100 year are established from 3.6.

— Based on Return Period Values.

Distribution parameters for an assumed distribution e.g. Weibull, are established using e.g. 3 equations (for 1, 10 and 100 year) with 3 unknowns (α, β and γ). This is, in principle, always feasible but engineering judgement applies as defining return period values inappropriately can lead to an unphysical Weibull pdf.

3.5.3 The wave climate at a given location may be characterised by a series of short-term sea states. Each short-term sea state may be characterised by H_s, T_p, and the main wave direction θ, measured relative to a given reference direction

The directional (i.e. versus θ) or omni-directional significant wave height may be specified as follows:

— A scatter diagram in terms of H_s, T_p, θ.

The fatigue analysis is based on the discrete sea-states reflected in the individual cells in the scatter diagram.

— A histogram in terms of (H_s, θ) versus probability of occurrence.

The fatigue analysis is based on the discrete events for H_s in the histogram. The corresponding peak period may be assumed on the form:

$$T_p = C_T\left(H_s\right)^{\alpha_T}$$

Where $6 \le C_T \le 8$ and $0.3 \le \alpha_T \le 0.5$ are location specific.

— A long term probability density function (pdf).

The corresponding Return Period Values (RPV) for 1, 10 and 100 year are established from 3.6.

— Based on Return Period Values.

The corresponding Weibull distribution is established from 3.6.2 using 3 equations (x_c for 1, 10 and 100 year) with 3 unknowns (α, β and γ). This is, in principle, always feasible but engineering judgement applies as defining return period values inappropriately can lead to an unphysical Weibull pdf.

3.6 Return period values

3.6.1 Return period values are to be used for ULS conditions. A Return Period Value (RPV) x_c is defined as:

$$F(x_c) = 1 - \frac{1}{N}$$

where N is the number of independent events in the return period (e.g. 100 year). For discrete directions, N may be taken as the total number of independent events times the sector probability.

The time between independent events depends on the environmental condition. For currents, this time is often taken as 24 hours, whereas the time between independent sea-states (described by H_s) normally may be taken as 3-6 hours.

3.6.2 For a Weibull distributed variable the return period value is given by:

$$x_c = \alpha\left(\ln(N)\right)^{1/\beta}+\gamma$$

3.6.3 In case the statistics are given in terms of a scatter diagram, a long term Weibull distribution (α, β, γ) is established from 3.5.1 using statistical moments derived directly from the scatter diagram as follows:

$$\mu = \sum_{H_S}\left(H_s\right)\cdot P_{H_S}$$

$$\sigma = \sqrt{\sum_{H_S}\left(H_s-\mu\right)^2\cdot P_{H_S}}$$

$$\delta = \frac{\sum_{H_S}\left(H_s-\mu\right)^3\cdot P_{H_S}}{\sigma^3}$$

where P_{Hs} is the discrete occurrence probability. The same principle applies for current histograms.

3.6.4 The return period value to be used for directional data is taken as the maximum projected flow velocity, i.e.:

$$\max_{i=1..n}\left(x_{c,i}\cdot R_D(\theta_{rel,i})/R_D(\theta_{rel}=0)\right)$$

where R_D is a reduction factor defined by 3.4.3, $\theta_{rel,i}$ is the relative direction between the pipeline direction and the flow direction for direction i.

4. Response Models

4.1 General

4.1.1 Amplitude response models are empirical models providing the maximum steady state VIV amplitude response as a function of the basic hydrodynamic and structural parameters. The response models provided herein have been derived based on available experimental laboratory test data and a limited amount of full-scale tests for the following conditions:

— in-line VIV in steady current and current dominated conditions
— cross-flow VIV induced in-line motion
— cross-flow VIV in steady current and combined wave and current conditions.

The response models are in agreement with the generally accepted concept of VIV.

4.1.2 In the response models, in-line and cross-flow vibrations are considered separately. Damage contributions from both first and second in-line instability regions in current dominated conditions are implicit in the in-line model. Cross-flow induced additional in-line VIV resulting in possible increased fatigue damage is considered in an approximate way. Cross-flow induced in-line VIV is relevant for all reduced velocity ranges where cross-flow VIV occurs.

4.1.3 In case of multi-mode response, i.e. when several vibration modes may be excited simultaneously in the same direction (in-line or cross-flow), the computational procedure given in Appendix A accounts for possible reductions in the response amplitude.

4.1.4 The amplitude response depends on a set of hydrodynamic parameters constituting the link between the environmental data and the Response Models:

— reduced velocity, V_R
— Keulegan-Carpenter number, KC
— current flow velocity ratio, α;
— turbulence intensity, I_c, see 3.2.11
— flow angle, relative to the pipe, θ_{rel}
— stability parameter, K_S.

Note that the Reynolds number, R_e, is not explicit in the evaluation of response amplitudes.

4.1.5 The reduced velocity, V_R, is defined as:

$$V_R = \frac{U_c + U_w}{f_n D}$$

where

f_n Natural frequency for a given vibration mode
U_c Mean current velocity normal to the pipe, see 3.4.
U_w Significant wave-induced flow velocity, see 3.4.
D Outer pipe diameter.

4.1.6 The Keulegan-Carpenter number is defined as:

$$KC = \frac{U_w}{f_w D}$$

where f_w is the (significant) wave frequency.

4.1.7 The current flow velocity ratio is defined by:

$$\alpha = \frac{U_c}{U_c + U_w}$$

4.1.8 The stability parameter, K_S, representing the damping for a given modal shape is given by:

$$K_S = \frac{4\pi m_e \zeta_T}{\rho D^2}$$

where

ρ Water density
ζ_T Total modal damping ratio
m_e Effective mass, see Sec.6.7.3.

4.1.9 The total modal damping ratio, ζ_T, comprises:

— structural damping, ζ_{str}, see Sec.6.2.11
— soil damping, ζ_{soil}. For screening purposes $\zeta_{soil} = 0.01$ may be assumed. For details, see 7.3.1
— hydrodynamic damping, ζ_h. For VIV within the lock-in region, the hydrodynamic modal damping ratio ζ_h is normally to be taken as zero, i.e. $\zeta_h = 0.00$.

4.2 Marginal fatigue life capacity

4.2.1 For **cross-flow** VIV, the marginal fatigue capacity against VIV in a single sea-state characterised by (H_s, T_p, θ) is defined by, see Sec.2.4:

$$T^{RM,CF}_{Hs,Tp,\theta} = \frac{1}{\int_0^\infty \frac{\left(f_v \cdot S^m_{CF}\right)}{\bar{a}} dF_{Uc}}$$

where

S_{CF} Cross-flow stress range defined in 4.4
f_v Vibration frequency, see 4.2.3
$\bar{a}$ Fatigue constant, depending on the relevant stress range, see Sec.2.4.3
m Fatigue exponent, depending on the relevant stress range, see Sec.2.4.3.

The integral $\int(...)\, dF_{u_c}$ indicates integration over the long-term distribution for the current velocity represented by a Weibull distribution or histogram.

4.2.2 For the **in-line** direction, the marginal fatigue capacity against VIV in a single sea-state characterised by (H_s, T_p, θ) is taken as:

$$T^{RM,IL}_{Hs,Tp,\theta} = \frac{1}{\int_0^\infty \frac{f_v \cdot \max\left(S_{IL}; \frac{S_{CF}}{2.5}\frac{A_{IL}}{A_{CF}}\right)^m}{\bar{a}} dF_{Uc}}$$

where

S_{IL} In-line stress range defined in 4.3
A_{IL} Stress due to unit diameter in-line mode shape deflection
A_{CF} Stress due to unit diameter cross-flow mode shape deflection.

The in-line stress range is taken as the maximum of:

— the in-line VIV stress range S_{IL}
— the in-line stress range corresponding to a figure **8** or half-moon motion, i.e., stress induced by 40% of the cross-flow induced VIV amplitude.

4.2.3 The dominating vibration frequency, f_v, is to be taken as:

— $f_v = f_{n,IL}$ for in-line VIV
— $f_v = f_{n,CF\text{-}RES}$ for cross-flow VIV
— $f_v = 2 \cdot f_{n,CF\text{-}RES}$ for cross-flow induced in-line motion.

where $f_{n,IL}$ denotes the in-line still-water vibration frequencies.

4.2.4 The cross-flow response frequency is obtained based on the updated added mass coefficient ($C_{a,\,CF\text{-}RES}$) due to cross-flow response using the following equation:

$$f_{n,CF-RES} = f_{n,CF}\sqrt{\frac{(\rho_s/\rho)+C_a}{(\rho_s/\rho)+C_{a,CF-RES}}}$$

where ρ_s/ρ is the specific mass ratio between the pipe mass (not including added mass) and the displaced water, and $f_{n,CF}$ is the n'th still water eigen frequency using the added mass according to C_a, see 6.9. The added mass coefficient due to cross-flow response ($C_{a,\,CF\text{-}RES}$) is shown in 4.5.

Guidance note:

The cross-flow response frequency is used for stress cycle counting in the fatigue calculation. However, it is also used to determine which of the in-line modes may be candidates for cross-flow induced in-line vibrations.

The reduced velocity and, thus, the VIV amplitude according to the response model is determined by the still water frequency as any potential change in added mass is accounted for in the response models.

---e-n-d---of---G-u-i-d-a-n-c-e---n-o-t-e---

4.3 In-line response model

4.3.1 The in-line response of a pipeline span in current dominated conditions is associated with either alternating or symmetric vortex shedding. Contributions from both the first in-line instability region and the second instability region are included in the model.

The in-line response model applies for all in-line vibration modes.

4.3.2 The amplitude response depends mainly on the reduced velocity, V_R, the stability parameter, K_S, the turbulence intensity, I_c, and the flow angle, θ_{rel} relative to the pipe. Mitigation effects from the seabed proximity, (e/D) are conservatively not included.

4.3.3 The in-line VIV induced stress range S_{IL} is calculated by the Response Model:

$$S_{IL} = 2 \cdot A_{IL} \cdot (A_Y / D) \cdot \psi_{\alpha,IL} \cdot \gamma_s$$

where

A_{IL} Unit stress amplitude (stress due to unit diameter in-line mode shape deflection)
$\psi_{\alpha,IL}$ Correction factor for current flow ratio α
γ_s Safety factor to be multiplied to the stress range.

4.3.4 (A_Y/D) is defined as the maximum in-line VIV response amplitude (normalised with D) as a function of V_R and K_S, see Figure 4-1. The corresponding standard deviation may be obtained as (A_Y /D)/√2.

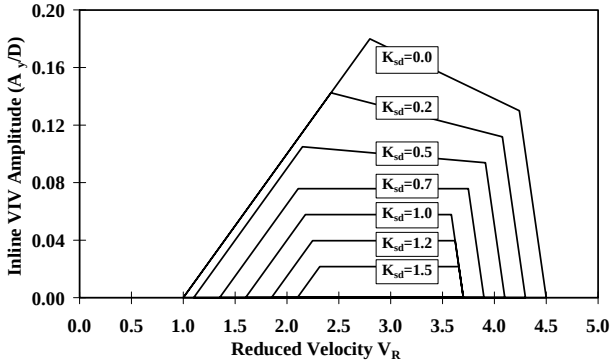

Figure 4-1
Illustration of the in-line VIV Response Amplitude versus V_R and K_S

4.3.5 The response model can be constructed from the co-ordinates in Figure 4-2:

$$V_{R,onset}^{IL} = \begin{cases} \left(\frac{1.0}{\gamma_{on,IL}}\right) & for \quad K_{sd} < 0.4 \\ \left(\frac{0.6+K_{sd}}{\gamma_{on,IL}}\right) & for \quad 0.4 < K_{sd} < 1.6 \\ \left(\frac{2.2}{\gamma_{on,IL}}\right) & for \quad K_{sd} > 1.6 \end{cases}$$

$$V_{R,1}^{IL} = 10 \cdot \left(\frac{A_{Y,1}}{D}\right) + V_{R,onset}^{IL}$$

$$V_{R,2}^{IL} = V_{R,end}^{IL} - 2 \cdot \left(\frac{A_{Y,2}}{D}\right)$$

$$V_{R,end}^{IL} = \begin{cases} 4.5 - 0.8\,K_{sd} & for\ K_{sd} < 1.0 \\ 3.7 & for\ K_{sd} \geq 1.0 \end{cases}$$

$$\left(\frac{A_{Y,1}}{D}\right) = \max\left(0.18 \cdot \left(1 - \frac{K_{sd}}{1.2}\right) \cdot R_{I\theta,1}; \left(\frac{A_{Y,2}}{D}\right)\right)$$

$$\left(\frac{A_{Y,2}}{D}\right) = 0.13 \cdot \left(1 - \frac{K_{sd}}{1.8}\right) \cdot R_{I\theta,2}$$

Guidance note:

In the evaluation of (A_Y/D) the design values for the reduced velocity and stability parameter shall be applied:

$$V_{Rd} = V_R\,\gamma_f$$
$$K_{sd} = \frac{K_s}{\gamma_k}$$

where γ_f and γ_k are safety factors related to the natural frequency and damping respectively. In addition, an onset safety factor is needed, see Sec.2.6.

---e-n-d---of---G-u-i-d-a-n-c-e---n-o-t-e---

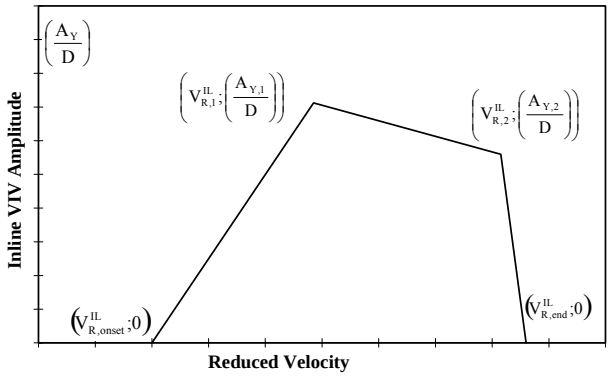

Figure 4-2
Response model generation principle.

4.3.6 The reduction factors, $R_{I\theta,1}(I_c,\theta_{rel})$ and $R_{I\theta,2}(I_c)$, account for the effect of the turbulence intensity and angle of attack (in radians) for the flow, see Figure 4-3.

$$R_{I\theta,1} = 1 - \pi^2\left(\frac{\pi}{2} - \sqrt{2}\cdot\theta_{rel}\right)\left(I_c - 0.03\right) \qquad 0 \le R_{I\theta,1} \le 1$$

$$R_{I\theta,2} = 1.0 - \frac{\left(I_c - 0.03\right)}{0.17} \qquad 0 \le R_{I\theta,2} \le 1$$

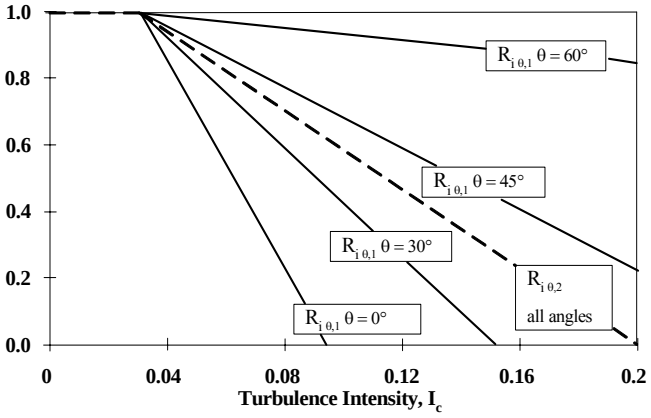

Figure 4-3
Reduction function wrt turbulence intensity and flow angle

4.3.7 $\psi_{\alpha,IL}$ is a reduction function to account for reduced in-line VIV in wave dominated conditions:

$$\psi_{\alpha,IL} = \begin{cases} 0.0 & for \quad \alpha < 0.5 \\ (\alpha - 0.5)/0.3 & for \quad 0.5 < \alpha < 0.8 \\ 1.0 & for \quad \alpha > 0.8 \end{cases}$$

Thus, if $\alpha < 0.5$, in-line VIV may be ignored.

4.4 Cross-flow response model

4.4.1 Cross-flow VIV are affected by several parameters, such as the reduced velocity V_R, the Keulegan-Carpenter number, KC, the current flow velocity ratio, α, the stability parameter, K_S, the seabed gap ratio, (e/D), the Strouhal number, S_t and the pipe roughness, (k/D), among others. Note that Reynolds number, Re, is not explicit in the model.

4.4.2 For steady current dominated flow situations, onset of cross-flow VIV of significant amplitude occurs typically at a value of V_R between 3.0 and 4.0, whereas maximum vibration levels occur at larger V_R values. For pipes with low specific mass, wave dominated flow situations or span scenarios with a low gap ratio, cross-flow vibration may be initiated for V_R between 2 and 3.

4.4.3 The cross-flow VIV induced stress range S_{CF} due to a combined current and wave flow is assessed using the following response model:

$$S_{CF} = 2 \cdot A_{CF} \cdot (A_Z / D) \cdot R_k \cdot \gamma_s$$

where

A_{CF}	Unit stress amplitude (stress due to unit diameter cross-flow mode shape deflection)
R_k	Amplitude reduction factor due to damping
γ_s	Safety factor to be multiplied on the stress range

The cross-flow VIV amplitude (A_Z/D) in combined current and wave flow conditions may be taken from Figure 4-4. The figure provides characteristic maximum values. The corresponding standard deviation may be obtained as (A_Z /D)/√2.

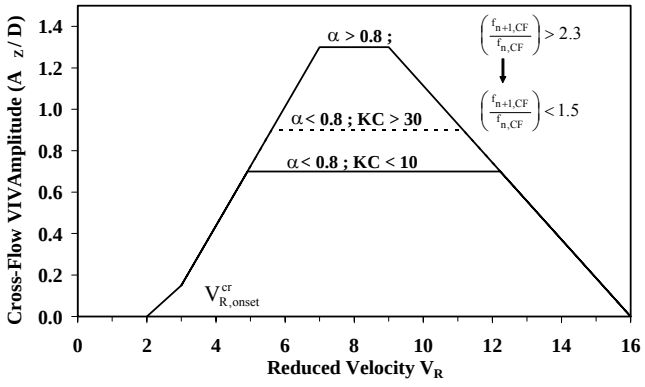

Figure 4-4
Basic cross-flow response model

4.4.4 The amplitude response (A_Z/D) as a function of α and KC can be constructed from, see Figure 4-5:

$$V_{R,onset}^{CF} = \frac{3 \cdot \psi_{proxi,onset} \cdot \psi_{trench,onset}}{\gamma_{on,CF}}$$

$$V_{R,1}^{CF} = 7 - \frac{(7 - V_{R,onset}^{CF})}{1.15} \cdot \left(1.3 - \frac{A_{Z,1}}{D}\right)$$

$$V_{R,2}^{CF} = V_{R,end}^{CF} - \left(\frac{7}{1.3}\right) \cdot \left(\frac{A_{Z,1}}{D}\right)$$

$$V_{R,end}^{CF} = 16$$

$$\left(\frac{A_{Z,1}}{D}\right) = \begin{cases} 0.9 & \alpha > 0.8 \quad \left(\frac{f_{n+1,CF}}{f_{n,CF}}\right) < 1.5 \\ 0.9 + 0.5 \cdot \left(\frac{f_{n+1,CF}}{f_{n,CF}} - 1.5\right) & \alpha > 0.8 \quad 1.5 \le \left(\frac{f_{n+1,CF}}{f_{n,CF}}\right) \le 2.3 \\ 1.3 & \alpha > 0.8 \quad \left(\frac{f_{n+1,CF}}{f_{n,CF}}\right) > 2.3 \\ 0.9 & \alpha \le 0.8 \quad KC > 30 \\ 0.7 + 0.01 \cdot (KC - 10) & \alpha \le 0.8 \quad 10 \le KC \le 30 \\ 0.7 & \alpha \le 0.8 \quad KC < 10 \end{cases}$$

$$\left(\frac{A_{Z,2}}{D}\right) = \left(\frac{A_{Z,1}}{D}\right)$$

$\left(\frac{f_{n+1,CF}}{f_{n,CF}}\right)$ is the cross-flow frequency ratio for two consecutive (contributing) cross flow modes.

Guidance note:

The maximum cross-flow response amplitude of 1.3 D is typically only applicable for current dominated cases with bending stiffness dominated lower half-wave symmetric modes e.g., for single span fundamental mode. For all other current dominated cases the maximum response amplitude is limited to 0.9 D.

---e-n-d---of---G-u-i-d-a-n-c-e---n-o-t-e---

Guidance note:

In the evaluation of (A_Z/D) the design values for the reduced velocity and stability parameter shall be applied:

$$V_{Rd} = V_R \, \gamma_f$$

where γ_f is safety factor related to the natural frequency.

---e-n-d---of---G-u-i-d-a-n-c-e---n-o-t-e---

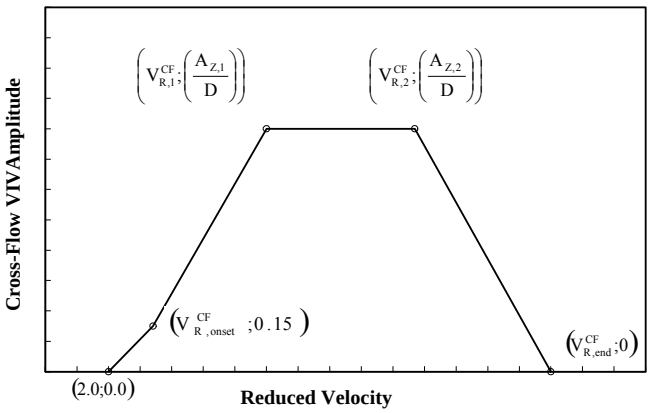

Figure 4-5
Response model generation principle

4.4.5 The reduced onset velocity for cross-flow VIV, $V_{R,onset}^{CF}$ depends on the seabed proximity and trench geometry, whereas the maximum amplitude is a function of α and KC.

4.4.6 $\psi_{proxi,onset}$ is a correction factor accounting for the seabed proximity:

$$\psi_{proxi,onset} = \begin{cases} \frac{1}{5}(4 + 1.25\frac{e}{D}) & for \ \frac{e}{D} < 0.8 \\ 1 & else \end{cases}$$

4.4.7 $\psi_{trench,onset}$ is a correction factor accounting for the effect of a pipe located in/over a trench:

$$\psi_{trench,onset} = 1 + 0.5\frac{\Delta}{D}$$

where Δ/D denotes a relative trench depth given by:

$$\frac{\Delta}{D} = \frac{1.25d - e}{D}$$
$$where \quad 0 \le \frac{\Delta}{D} \le 1$$

The trench depth d is to be taken at a width equal to 3 outer diameters. $\Delta/D = 0$ corresponds to a flat seabed or a pipe located in excess of D/4 above the trench, i.e. the pipe is not affected by the presence of the trench, see Figure 4-6. The restriction $\Delta/D < 1.0$ is applied in order to limit the relative trench depth.

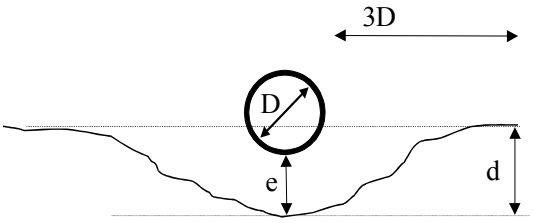

Figure 4-6
Definition of trench factor

4.4.8 The characteristic amplitude response for cross-flow VIV may be reduced due to the effect of damping. The reduction factor, R_k is given by:

$$R_k = \begin{cases} 1 - 0.15K_{sd} & \text{for } K_{sd} \le 4 \\ 3.2K_{sd}^{-1.5} & \text{for } K_{sd} \succ 4 \end{cases}$$

4.4.9 The normalised amplitude curves in Figure 4-4 to a large degree embody all available test results. In addition, the following comments apply:

— The response for small gap ratio (e/D<< 1) is associated with one-sided vortex shedding and may not be characterised by VIV parameters as V_R and KC. However, the indicated response curve is considered conservative in general.
— The response for low KC numbers in the cross-flow response model is not in a narrow sense related to the VIV phenomenon but rather linked to wave-induced water particle motions. Typical maximum response at V_R between 2.5 and 3.0 occurs at $T_u/T_0 \approx 2$. T_u is the wave-induced flow period at pipe level and T_0 is the natural period.

4.4.10 Potential vibrations at low KC numbers must be accounted for and care should be observed in case:

$$V_R > \frac{KC}{3 \cdot (1 - \alpha)} \quad and \quad 3 < KC < 9$$

This corresponds to rare cases where $T_u < 3T_0$. If violated, the criticality should be evaluated using an appropriate force model.

Guidance note:

The relevance of 4.4.10 should be checked especially for shallow water free span pipelines, and it may require that full fatigue analysis is performed if the 1-year significant wave-induced flow at pipe level is larger than half the 100-year current velocity at pipe level.

It is also possible to apply the screening criteria in the same way as the traditional on-set criterion in order to establish conservative allowable free span lengths even though the above mentioned wave effect criterion is violated.

If the flow is current dominated, the free span may be assessed by adding a characteristic wave-induced flow component to the current velocity as expressed in the in-line VIV screening criterion.

If the flow has a stronger component from the waves, then generally a full fatigue analysis has to be performed. However, the in-line VIV screening criterion may still be used provided that a quasi-static Morison force calculation shows that the fatigue due to direct wave action could be neglected or is insignificant compared to in-line VIV fatigue.

---e-n-d---of---G-u-i-d-a-n-c-e---n-o-t-e---

4.5 Added mass coefficient model

4.5.1 The calculation of added mass coefficient described in this section is for the calculation of the cross-flow response frequency of the dominant mode only.

It should be noted that the response models discussed in this section, have the effect of the added mass built-into them, i.e. they are plotted using the reduced velocity calculated with the still water natural frequency and associated added mass.

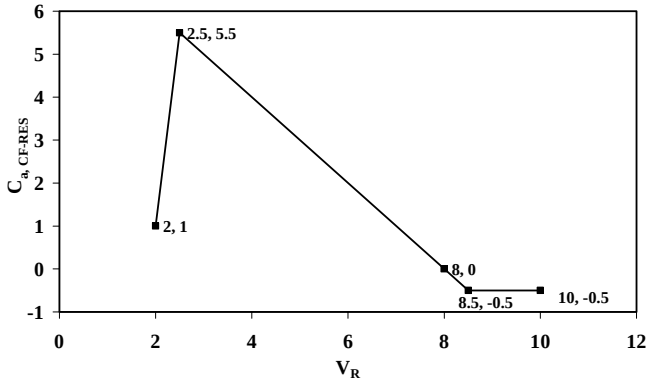

Figure 4-7
Added mass coefficient $C_{a, CF-RES}$ as a function of reduced velocity

4.5.2 The added mass during VIV will be different from the still water added mass, which is applied during the initial eigen value analysis. The added mass coefficient is applied to correct the still water cross-flow eigen frequency to the cross-flow response frequency.

Guidance note:

This added mass model is in a narrow sense only valid when the mass ratio is in the order of 1.4, but may be used also for other mass ratios if better information is not available.

---e-n-d---of---G-u-i-d-a-n-c-e---n-o-t-e---

Guidance note:

The added mass coefficient formulation for VR < 2.5 is not important, since the cross-flow response amplitude are very small (A/D is O (0.1)) in this range.

---e-n-d---of---G-u-i-d-a-n-c-e---n-o-t-e---

5. Force Model

5.1 General

5.1.1 In principle, force models may be used for both vortex induced and direct wave and current dominated loads if appropriate formulations of force models exist and reliable and consistent data are available for calibration. For cross-flow VIV, generally applicable force models do not exist and empirical response models presented in Sec.4.4 reflecting observed pipeline response in a variety of flow conditions is at present superior.

5.1.2 A force model based on the well-known Morison's equation for direct in-line loading is considered herein. Both time domain (TD) and frequency domain (FD) solutions are allowed. A time domain solution may account for all significant non-linearities but is in general very time consuming if a large number of sea-states are to be analysed. For fatigue analyses, a frequency domain solution (if thoroughly verified) is more tractable since it facilitates analyses of a very large number of sea-states at a small fraction of the time required for a time domain solution.

5.1.3 In this document, a complete frequency domain approach for short-term fatigue analyses is presented. Recommended procedures for state-of-the-art time domain short-term damage calculation may be found in DNV-OS-F201. A simplified assessment method is given in 5.3.

5.2 FD solution for in-line direction

5.2.1 The recommended frequency domain solution for the short term- fatigue damage due to combined current and direct wave actions in a single sea-state is based on:

- Palmgren-Miner approach using SN-curves
- linearisation scheme for drag term in the Morison equation based on conservation of damage
- effect of co-linear mean current included in linearisation term
- narrow banded fatigue damage with semi-empirical correction to account for wide-band characteristic.

The formulation presented in this document has been successfully verified against comprehensive time domain simulations using Rain flow counting techniques, see e.g. Mørk & Fyrileiv, (1998). The formulation is based on the following assumptions:

- the main damage contribution comes from the lowest natural mode, i.e. the excitation frequency is far from the natural frequency for the higher order modes
- the effective mass, m_e, and standard deviation of the flow velocity σ_U is invariant over the free span length, i.e. for span length less than the dominant wavelength.

5.2.2 The short term fatigue capacity against direct wave actions in a single sea-state characterised by (H_S, T_p, θ) is given in the following form:

$$T^{FM}_{H_S,T_P,\theta} = \frac{\overline{a_1}\cdot S^{-m_1}}{f_v \cdot \kappa_{RFC}(m_1)} \times \left[G_1\left\{\left(1+\frac{m_1}{2}\right),\left(\frac{S_{sw}}{S}\right)^2\right\} + \chi \cdot G_2\left\{\left(1+\frac{m_2}{2}\right),\left(\frac{S_{sw}}{S}\right)^2\right\}\right]^{-1}$$

$$\chi = \frac{\kappa_{RFC}(m_2)}{\kappa_{RFC}(m_1)}\frac{\overline{a_1}}{\overline{a_2}} S^{(m_2-m_1)}$$

$$S = 2\sqrt{2}\,\sigma_s \cdot \gamma_s$$

where

σ_S Standard deviation of stress amplitude
f_v Vibration frequency
$\overline{a_1}$, $\overline{a_2}$ Fatigue constants, see Sec.2.4.3
m_1 , m_2 Fatigue exponent, see Sec.2.4.3
S_{sw} Stress range, for which change in slope occurs, see 2.4.3

$G_1(\varphi, x) = \int_x^\infty e^{-t}\, t^{\varphi-1}\, dt$ is the Complementary incomplete Gamma function

$G_2(\varphi, x) = \int_0^x e^{-t}\, t^{\varphi-1}\, dt$ is the Incomplete Gamma function

γ_s Safety factor on stress range, see Sec.2.6

5.2.3 The standard deviation of the wave-induced stress amplitude σ_S is given by the square root of the spectral moment of the 0th order defined by 5.2.6.

$$\sigma_S = \sqrt{M_0}$$

5.2.4 The characteristic vibration frequency of considered pipe stress response, f_v, is taken equal to the mean up-crossing frequency defined by:

$$f_v \approx \frac{1}{2\pi}\sqrt{\frac{M_2}{M_0}}$$

M_0 and M_2 is defined by 5.2.6.

5.2.5 The rain flow counting correction factor, κ_{RFC}, accounts for the "exact" wide-banded damage, i.e. correcting the implicit narrow-banded Rayleigh assumption for the stress amplitudes to provide results similar to those arising from a state-of-the-art rain flow counting technique. The Rain Flow Counting factor κ_{RFC} is given by:

$$\kappa_{RFC}(m) = a_\kappa + (1 - a_\kappa)(1 - \varepsilon)^{b_\kappa}$$

where

$$a_\kappa = 0.926 - 0.033m$$

$$b_\kappa = 1.587m - 2.323$$

The bandwidth parameter ε is defined as:

$$\varepsilon = \sqrt{1 - \frac{M_2^2}{M_0 M_4}}$$

The stress process is narrow-banded for $\varepsilon \to 0$ and broad banded for $\varepsilon \to 1$ (in practice the process may be considered broad-banded for ε larger than 0.6).

5.2.6 The n^{th} response spectral moment is given by:

$$M_n = \int_0^\infty \omega^n\, S_{SS}(\omega) d\omega$$

where $S_{SS}(\omega)$ is the one-sided stress response spectral density function given by:

$$S_{SS}(\omega) = \frac{R_D^2 \cdot \left(b^2 g_D^2 + \omega^2 g_I^2\right) \cdot G^2(\omega) \cdot S_{\eta\eta}(\omega) \times \sum \lambda_{max}^2}{m_e^2\left((\omega_n^2 - \omega^2)^2 + (2\zeta_T \omega_n \omega)^2\right)}$$

where

R_D Factor accounting for wave spreading and direction, see Sec.3.4.3
b Linearisation constant, see 5.2.8
g_D Drag force term, see 5.4.1
g_I Inertia force term, see 5.4.1
$G(\omega)$ Frequency transfer function, see Sec.3.3
$S_{\eta\eta}$ Single-sided wave elevation spectrum, see Sec.3.3
ω_n $= 2\pi f_n/\gamma_f$ is the lowest angular natural frequency
ζ_T Total damping ratio from:

— structural damping, see Sec.6.2.10
— soil damping, see Sec.7.3
— hydrodynamic damping, see Sec.5.2.9.

m_e Effective mass per unit length incl. added mass, see 6.7.3

5.2.7 λ_{max} is an equivalent stress factor given by:

$$\lambda_{max} = (1 + CSF)\frac{(D_s - t)E}{2}\lambda_1 \max_L\left(\frac{\partial^2 \phi_1}{\partial x^2}\right)$$

$\phi_1(x)$ 1st mode shape
E Young's modulus
CSF Concrete stiffness factor, see Sec.6.2.5
D_s Outer steel pipe diameter
t Pipe wall thickness
L Length of mode shape
λ_1 Mode shape weighting factor given by:

$$\lambda_1 = \frac{\int_0^L \phi_1(x)dx}{\int_0^L \phi_1^2(x)dx}$$

λ_1 is typically in the order of 1.3.

In lieu of more detailed data, λ_{max} may be taken as:

$$\lambda_{max} = \frac{A_{IL}}{D}\lambda_1$$

where A_{IL} is given by Sec.6.7.4.

5.2.8 The linearisation constant b is given by:

$$b = 2.11 \cdot \sigma_u \cdot g_c\left(\frac{U_c}{\sigma_u}\right)$$

where U_c is the mean current and $\sigma_u = U_w/2$ is the standard deviation of the wave-induced flow velocity. $g_c(\bullet)$ is a correction function accounting for the effect of a steady current given by:

$$g_c(x) = \sqrt{2\pi}\left(\varphi(x) + x\cdot\left(\Phi(x) - \frac{1}{2}\right)\right);$$

$$\varphi(x) = \frac{1}{\sqrt{2\pi}} e^{-\frac{1}{2}x^2}$$

$$\Phi(x) = \int_{-\infty}^{x} \varphi(x)\,dx$$

$\varphi(x)$ is the Gaussian probability density function and $\Phi(x)$ is the corresponding distribution function.

5.2.9 The (linearised) hydrodynamic damping ratio ζ_h is given by:

$$\zeta_h = \frac{1}{\sqrt{2\pi}} \frac{\sigma_u\, g_D}{m_e\, f_n} g_c\left(\frac{U_c}{\sigma_U}\right)\lambda_1$$

5.3 Simplified fatigue assessment

5.3.1 In situations where quasi-static stress response can be assumed (when the wave period is far larger than the natural vibration period of the span), a simplified fatigue assessment may be tractable rather than a complete time domain or frequency domain approach.

5.3.2 In such cases, the short term fatigue capacity against direct wave actions in a single sea-state characterised by (H_S, T_P, θ) may be estimated as follows: (See 2.4.5)

$$T^{FM}_{H_S,T_P,\theta} = \bar{a}\cdot S^{-m} T_u$$

where S is the quasi-static stress range response from a direct regular wave load (H_s and T_u) using Morison's equation. T_u is the mean zero upcrossing period in Sec.3.3.6.

5.4 Force coefficients

5.4.1 The force P(x,t) per unit length of a pipe free span is represented by the Morison's equation. Assuming that the velocity of the structure is not negligible compared with the water particle velocity Morison's equation reads:

$$P(x,t) = g_D\left(U - \dot{y}\right)\left|U - \dot{y}\right| + g_I \dot{U} - C_a \frac{\pi}{4}\rho D^2 \ddot{y}$$

where

ρ Water density
D Outer pipe diameter
U Instantaneous (time dependent) flow velocity
y Pipe lateral displacement
g_D = $0.5\rho D C_D$ is the drag force term

g_I = $\frac{\pi}{4}\rho D^2 C_M$ is the inertia force term

5.4.2 The added mass term in the Morison equation

$$C_a \frac{\pi}{4}\rho D^2 \ddot{y}$$

is assumed implicit in the effective mass m_e, see Sec.6.9.1.

5.4.3 The drag coefficient C_D and inertia coefficient C_M to be used in Morison's equation are functions of :

— the Keulegan Carpenter number, KC
— the current flow ratio, α;
— the gap ratio, (e/D)
— the trench depth, (Δ/D)
— Reynolds number, R_e
— the pipe roughness, (k/D).

In addition also the cross-flow vibration level, (A_y/D) influences the drag coefficient. Supercritical flow is assumed, hence there no further dependency of the Reynolds number is considered.

The drag coefficient C_D is to be taken as:

$$C_D = C_D^0(k/D)\cdot \psi^{CD}_{KC,\alpha}\cdot \psi^{CD}_{proxi}\cdot \psi^{CD}_{trench}\cdot \psi^{CD}_{VIV}$$

5.4.4 $C_D^0(k/D)$ is the basic drag coefficient for steady flow as a function of roughness k/D.

$$C_D^0(k/D) = \begin{cases} 0.65 & ;\ k/D < 10^{-4}\ \text{(smooth)} \\ 0.65\cdot\left(\frac{29}{13} + \frac{4}{13}\log_{10}(k/D)\right) & ;\ 10^{-4} < k/D < 10^{-2} \\ 1.05 & ;\ k/D > 10^{-2}\ \text{(rough)} \end{cases}$$

In lieu of detailed documentation of the surface roughness the values in Table 5-1 may be applied for the absolute roughness, k.

Table 5-1 Surface roughness

Pipe surface	*k [metres]*
Steel, painted	10^{-6}
Steel, un-coated (not rusted)	10^{-5}
Concrete	1/300
Marine growth	1/200 → 1/20

Note that the roughness, k/D, to be used in 5.4.4 is the ratio between, k, and the outer diameter, D, of the pipe.

5.4.5 $\psi^{CD}_{KC,\alpha}$ is a correction factor accounting for the unsteadiness of the flow, including effects of Keulegan-Carpenter number KC and the current flow ratio α:

$$\psi^{CD}_{KC,\alpha} = \begin{cases} 0.85 + \frac{6}{KC} - \frac{\alpha}{2} & \alpha \le 0.5 \\ 0.6 + \frac{6}{KC} & \alpha > 0.5 \end{cases} \qquad 5 < KC < 40$$

For KC > 40, the term 6/KC in the formula above shall be substituted by 0.15.

The drag load is often of small practical importance for small KC values and $\psi^{CD}_{KC,\alpha}$ may be interpolated for completeness for KC < 5.

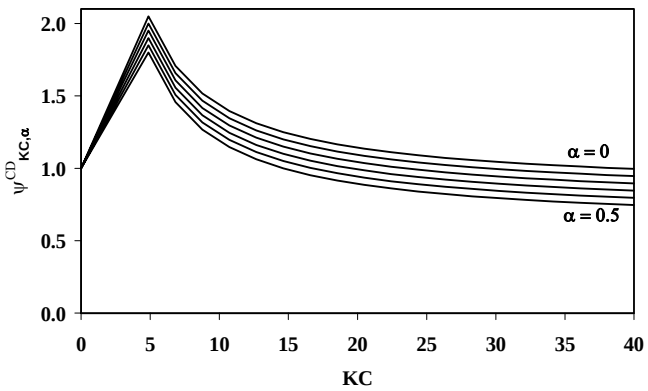

Figure 5-1
Correction factor $\psi^{CD}_{KC,\alpha}$

5.4.6 ψ^{CD}_{proxi} is a correction factor accounting for the seabed proximity:

$$\psi^{CD}_{proxi} = \begin{cases} 0.9 + \dfrac{0.5}{(1+5\cdot(e/D))} & \text{for } e/D < 0.8 \\ 1 & \text{else} \end{cases}$$

5.4.7 ψ^{CD}_{trench} is a correction factor accounting for the effect of a pipe in a trench:

$$\psi^{CD}_{trench} = 1 - \frac{2}{3}\left(\frac{\Delta}{D}\right)$$

Δ/D is the relative trench depth given by Sec.4.4.7.

5.4.8 ψ^{CD}_{VIV} is an amplification factor due to cross-flow vibrations, i.e.

$$\psi^{CD}_{VIV} = 1 + 1.043\left(\sqrt{2}\,\frac{A_z}{D}\right)^{0.65}$$

5.4.9 The inertia coefficient C_M is to be taken as:

$$C_M = C_{M,0}\cdot\psi^{CM}_{k}\cdot\psi^{CM}_{proxi}\cdot\psi^{CM}_{trench}$$

5.4.10 $C_{M,0}$ is the basic inertia coefficient for a free concrete coated pipe taken as, see Figure 5-2:

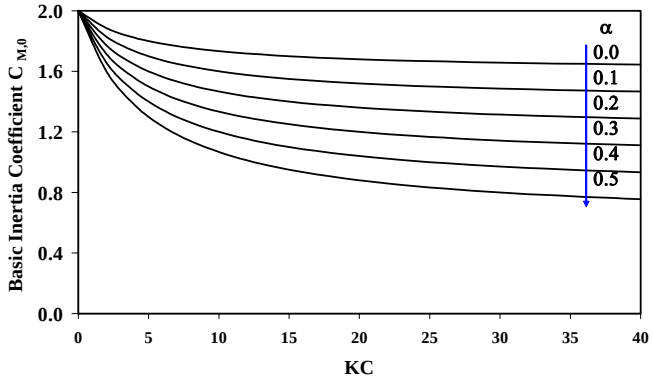

Figure 5-2
Basic inertia coefficient $C_{M,0}$ versus KC and α

$$C_{M,0} = f(\alpha) + \frac{5\cdot(2 - f(\alpha))}{(KC + 5)}$$

$$f(\alpha) = \begin{cases} 1.6 - 2\cdot\alpha & \alpha \le 0.5 \\ 0.6 & \alpha \succ 0.5 \end{cases}$$

5.4.11 ψ^{CM}_{k} is a correction factor accounting for the pipe roughness:

$$\psi^{CM}_{k} = 0.75 - 0.434\log\left(\frac{k}{D}\right)$$

5.4.12 ψ^{CM}_{proxi} is a correction factor accounting for the seabed proximity:

$$\psi^{CM}_{proxi} = \begin{cases} 0.84 + \dfrac{0.8}{(1+5\cdot(e/D))} & \text{for } e/D < 0.8 \\ 1 & else \end{cases}$$

5.4.13 ψ^{CM}_{trench} is a correction factor accounting for the effect of a pipe in a trench:

$$\psi^{CM}_{trench} = 1 - \frac{1}{3}\left(\frac{\Delta}{D}\right)$$

Δ/D is the relative trench depth given by Sec.4.4.7.

6. Structural Analysis

6.1 General

6.1.1 The following tasks are normally required for assessment of free spans:

- structural modelling
- modelling of pipe-soil interaction
- load modelling
- a static analysis to obtain the static configuration of the pipeline
- an eigen value analysis which provides natural frequencies and corresponding modal shapes for the in-line and cross-flow vibrations of the free spans
- a response analysis using a response model or a force model in order to obtain the stress ranges from environmental actions.

6.2 Structural modelling

6.2.1 The structural behaviour of the pipeline shall be evaluated by modelling the pipeline, seabed and relevant artificial supports and performing static and dynamic analyses. This section presents requirements for the structural modelling.

Soil-pipe interactions are treated in Sec.7.

6.2.2 A realistic characterisation of the cross-sectional behaviour of a pipeline can be based on the following assumptions:

- the pipe cross-sections remain circular and plane
- the stresses may be assumed constant across the pipe-wall thickness
- long term fatigue damage calculations may be based on actual/anticipated variation in pipe wall thickness over the design life of the free span (if detailed information is not available the calculation is to be performed using non-corroded cross section values for effective axial force and corroded cross section values for stresses)
- the application of this document is limited to elastic response, hence plasticity models and effects of two-dimensional state of stress (axial and hoop) on bending stiffness need not be considered.

6.2.3 The effect of coating is generally limited to increasing submerged weight, drag forces, added mass or buoyancy. The positive effect on the stiffness and strength, see 6.2.5, is normally to be disregarded. If the contribution of the coating to the structural response is considered significant, appropriate models shall be used.

6.2.4 Non-homogeneity of the bending stiffness along the pipe, due to discontinuities of the coating across field joints or other effects, may imply strain concentrations that shall be taken into account.

6.2.5 The stiffening effect of concrete coating may be accounted for by:

$$CSF = k_c\left(\frac{EI_{conc}}{EI_{steel}}\right)^{0.75}$$

where CSF denotes the stiffness of concrete coating relative to the steel pipe stiffness and (1 + CSF) is the stress concentration factor due to the concrete coating and localised bending. The

parameter k_c is an empirical constant accounting for the deformation/slippage in the corrosion coating and the cracking of the concrete coating. The value of k_c may be taken as 0.33 for asphalt and 0.25 for PP/PE coating.

In case the increased stiffness effect is utilised, the increased bending stresses due to field joints must also be accounted for.

The CSF given above is assumed valid for all relevant pipe diameters, D/t-ratios and concrete strengths, f_{cn}, provided that that the pipe joint length exceeds 12 m, the field joint length is 0.5-1.0m and the concrete coating thickness does not exceed 150 mm.

6.2.6 In lieu of detailed data, it is conservative to assume that a girth weld is present in the most heavily loaded cross-section. This is also a basis for the concrete stiffening effect given above.

6.2.7 The cross-sectional bending stiffness of the concrete coating, EI_{conc}, is the initial, uncracked stiffness. Young's modulus for concrete may be taken as:

$$E_{conc} = 10000 \cdot f_{cn}^{0.3}$$

where f_{cn} is the construction strength of the concrete. Both E_{conc} and f_{cn} are to be in N/mm^2.

6.2.8 The boundary conditions applied at the ends of the pipeline section modelled shall adequately represent the pipe-soil interaction and the continuity of the pipeline. Sufficient lengths of the pipeline at both sides of the span must be included in the model to account for the effects of side spans, if relevant.

6.2.9 The element length to be used in a finite element model is dictated by the accuracy required. If the stress ranges are to be derived from the mode shapes, see 6.7.4, the accuracy of the stress ranges becomes strongly affected by the element length, especially at the span shoulders.

Ideally the maximum element length should be found by reducing the length until the results (natural frequencies and stresses) converge towards constant values. In practice this may be difficult to perform, and, as guidance, the element length should be in the order of the outer diameter of the pipeline (1D). However, higher order modes and/or short spans ($L/D_s < 30$) may require shorter elements.

6.2.10 In order to obtain realistic rotational pipe-soil stiffness, contact should be ensured between at least two nodes at each span shoulder by using a sufficiently short element length or by other means.

6.2.11 Structural damping is due to internal friction forces of the pipe material and depends on the strain level and associated deflections. If no information is available, a structural modal damping ratio of

$$\zeta_{str} = 0.005$$

can be assumed. If concrete coating is present, the sliding at the interface between concrete and corrosion coating may further increase the damping to typically 0.01 - 0.02.

6.2.12 It is recommended to verify the finite element modelling and the post-processing by comparing the results from the finite element analysis with the approximate response quantities of 6.7 for a single span with zero effective axial force and $L/D_s = 60$. The in-line and cross-flow natural frequencies and stress ranges shall show similar values within ±5%.

6.2.13 ULS conditions may require a more refined pipe-soil modelling than the linearised eigen value analysis due to potential sliding at the span supports.

6.3 Functional loads

6.3.1 The functional loads which shall be considered are:

— weight of the pipe and internal fluid
— external and internal fluid pressure
— thermal expansion and contraction
— residual installation forces.

6.3.2 Response calculations must account for the relevant sequence of load application, if important.

6.4 Static analysis

6.4.1 The static configuration is to be determined for the following conditions if relevant:

— as-laid condition
— flooded condition
— pressure test condition
— operating condition.

6.4.2 The static analysis should normally account for non-linear effects such as:

— large displacements (geometric non-linearity)
— soil non-linear response
— loading sequence.

6.4.3 The stiffness of the pipeline consists of material stiffness and geometrical stiffness. The geometrical stiffness is governed by the effective axial force, S_{eff}. This force is equal to the true steel wall axial force, N_{tr}, with corrections for the effect of external and internal pressures:

$$S_{eff} = N_{tr} - p_i A_i + p_e A_e$$

N_{tr}	"True" steel wall axial force
p_i	Internal pressure
p_e	External pressure
A_i	Internal cross section area of the pipe
A_e	External cross section area of the steel pipe

The effective axial force in a span is difficult to estimate due to uncertainties in operational temperature and pressure, residual lay tension and axial force relaxation by sagging, axial sliding (feed-in), lateral buckling, multi-spanning and significant seabed unevenness. All these effects should be considered and taken into account if relevant. The most reliable method to estimate the effective axial force is use of non-linear FE analysis.

As boundary values, the effective axial force for a completely unrestrained (axially) pipe becomes:

$$S_{eff} = 0$$

while for a totally restrained pipe the following effective axial force applies (if pipe considered thin-walled):

$$S_{eff} = H_{eff} - \Delta p_i A_i (1 - 2\nu) - A_s E \Delta T \alpha_e$$

H_{eff}	Effective lay tension
Δp_i	Internal pressure difference relative to laying, see DNV-OS-F101
A_s	Pipe steel cross section area
ΔT	Temperature difference relative to laying
α_e	Temperature expansion coefficient, may be temperature dependent

Guidance note:

Using the expression for totally restrained pipe given above may lead to over-conservative fatigue results for pipelines on very uneven seabed with several long spans and for pipelines experiencing lateral buckling/snaking.

In such cases the structural response quantities must be based on refined, non-linear FE analyses.

---e-n-d---of---G-u-i-d-a-n-c-e---n-o-t-e---

6.4.4 In this document, the static environmental loads are confined to those from near bottom current. If the load is much smaller than the vertical functional loads, then it may be disregarded in the analysis. However, for light pipes or long span lengths it should be considered if relevant.

6.4.5 Load history effects such as the lay tension and submerged weight during installation will influence the static deflection and stresses which are mainly determined by the submerged weight and effective axial force in the phase considered.

Furthermore, the span geometry such as inclination of the span shoulders will have a significant influence on the static stresses and deflection. For this reason, the static response should be based on survey results (measured deflections) and/or FE analysis if considered as critical for the span assessment.

6.4.6 In addition to the static penetration into the soil due to the submerged weight of the pipeline, the penetration may increase due to effects from laying, erosion processes and self-burial.

6.5 Eigen value analyses

6.5.1 The aim of eigen value analyses is to calculate the natural frequencies and corresponding stress due to associated mode shapes. The analysis is normally complex and depends on:

- the temporal classification (scour or unevenness induced free span)
- the morphological classification (single or multispan)
- the pipeline condition (i.e. as-laid, water-filled, pressure test and operation)
- the pipe and soil properties
- the effective axial force and the initial deflected shape after laying
- the loading history and axial displacement ("feed-in") of the pipe.

6.5.2 In general, it is recommended that the response quantities be assessed using non-linear FE-analyses conducted over an appropriate stretch of the pipeline, see 6.6.

6.5.3 Approximate response quantities may be applied under certain limitations, see 6.7.

6.6 FEM based response quantities

6.6.1 Using an FE-approach, the following comments apply:

- the eigen value analysis shall account for the static equilibrium configuration
- in the eigen value analysis, a consistent linearisation of the problem must be made
- the pipe-soil linearisation should be validated
- the effect of geometric non-linearity on the dynamic response should be assessed
- the span support may be assumed invariant during Vortex-Induced Vibrations (VIV) but may change due to effects from direct wave loading.

6.6.2 For analysis of a pipeline stretch with several spans and especially with interacting spans, special care must be paid to the determination of the eigen values and associated eigen vectors. This is due to the potential occurrence of very close eigen values, especially with respect to the identification of correct eigen vectors.

6.7 Approximate response quantities

6.7.1 The approximate response quantities specified in this section may be applied for free span assessment provided:

- Conservative assumptions are applied with respect to span lengths, soil stiffness and effective axial force.
- The span is a single span on a relatively flat seabed, i.e. the span shoulders are almost horizontal and at the same level.
- The symmetrical mode shape dominates the dynamic response (normally relevant for the vertical, cross-flow response only). Here the following limits apply:

$$L/D_s < 140$$
$$\delta/D < 2.5$$

  Note that these are not absolute limits, the shift in cross-flow response from the symmetrical to the unsymmetrical mode will depend on the sagging and the levelling/inclination of the span shoulders. In cases where a shift in the cross-flow response is considered as likely, the structural response of the span should be assessed by using FE analysis including all important aspects
- Bar buckling does not influence the response, i.e.

$$S_{eff}/P_{cr} > -0.5$$

- A sensitivity study is performed in order to quantify the criticality of the assumptions.
- The approach is not applicable for multi-spanning pipelines.

Approximate response quantities are considered relevant in performing efficient screening of FE or survey results in order to identify critical spans to be assessed with methods that are more accurate, see Fyrileiv & Mørk, (1998).

6.7.2 The fundamental natural frequency (first eigen frequency) may be approximated by:

$$f_1 \approx C_1 \cdot \sqrt{1+CSF} \sqrt{\frac{EI}{m_e L_{eff}^4} \cdot \left(1+\frac{S_{eff}}{P_{cr}}+C_3\left(\frac{\delta}{D}\right)^2\right)}$$

where

$C_1 - C_3$	Boundary condition coefficients
E	Youngs modulus for steel
I	Moment of inertia for steel
CSF	Concrete stiffness enhancement factor
L_{eff}	Effective span length, see 6.7.9
m_e	Effective mass, see below
D	Outer diameter of pipe
P_{cr}	Critical buckling load = $(1+CSF)C_2\pi^2EI/L_{eff}^2$ (positive sign)
δ	Static deflection, normally ignored for in-line direction).
S_{eff}	Effective axial force (negative in compression), see 6.4

6.7.3 The effective mass, m_e, is defined by

$$m_e = \left(\frac{\int_L m(s)\phi^2(s)ds}{\int_L \phi^2(s)ds} \right)$$

where $\phi(s)$ is the assumed mode shape satisfying the boundary conditions and m(s) is the mass per unit length including struc-

tural mass, added mass and mass of internal fluid.

6.7.4 The unit diameter stress amplitude (stress due to unit outer diameter mode shape deflection) associated with the fundamental frequency may be calculated by:

$$A_{IL/CF} = (1+CSF)\frac{1}{2} D\, E\, (D_s - t)\frac{\partial^2 \phi}{\partial x^2}\left(1+\left(\frac{\partial \phi}{\partial x}\right)^2\right)^{-3/2}$$

where D_s is the steel pipe diameter, t is the wall thickness and D is the outer pipe diameter (including any coating).

6.7.5 In lieu of detailed information, the maximum (unit diameter) stress amplitude $A_{IL/CF}$ may be estimated as:

$$A_{IL/CF} = C_4 (1+CSF)\frac{D\cdot(D_s - t)\cdot E}{L_{eff}^2}$$

where t is the steel pipe wall thickness and C_4 is a boundary condition coefficient.

6.7.6 The static bending moment may be estimated as:

$$M_{static} = C_5 \frac{q\cdot L_{eff}^2}{\left(1+\frac{S_{eff}}{P_{cr}}\right)}$$

where q represents the loading, i.e. the submerged weight of the pipe in the vertical (cross-flow) direction and/or the drag loading in the horizontal (in-line) direction, see Sec.5.4.1.

Note that:

- L_{eff} shall be calculated using the static soil stiffness in the L_{eff}/L calculation.
- Due to historical effects and the local seabed geometry, there is a large uncertainty associated with this simplified expression, see 6.4.5.
- The term S_{eff}/P_{cr} becomes negative when the effective axial force is in compression since P_{cr} is defined as positive.

6.7.7 In case the static deflection is not given by direct measurement (survey) or estimated by accurate analytical tools, it may be estimated as:

$$\delta = C_6 \frac{q\cdot L_{eff}^4}{EI\cdot(1+CSF)}\frac{1}{\left(1+\frac{S_{eff}}{P_{cr}}\right)}$$

where C_6 is a boundary condition coefficient.

- L_{eff} shall be calculated using the static soil stiffness in the L_{eff}/L calculation.
- Due to historical effects and the local seabed geometry, there is a large uncertainty associated with this simplified expression, see 6.4.5.

6.7.8 The coefficients C_1 to C_6 are given in Table 6-1 for different boundary conditions. For multi-spanning scenarios, these coefficients should not be used and a dedicated FE-analysis is recommended.

Table 6-1 Boundary conditions coefficients

	Pinned-Pinned [2]	Fixed-Fixed [3]	Single span on seabed
C_1	1.57	3.56	3.56
C_2	1.0	4.0	4.0
C_3	0.8 [1]	0.2 [1]	0.4 [1]
C_4	4.93	14.1	Shoulder: $14.1(L/L_{eff})^2$ Mid-span: 8.6
C_5	1/8	1/12	Shoulder:[4] $\frac{1}{18(L_{eff}/L)^2 - 6}$ Mid-span: 1/24
C_6	5/384	1/384	1/384

1) Note that $C_3 = 0$ is normally assumed for in-line if the steady current is not accounted for.

2) For pinned-pinned boundary condition L_{eff} is to be replaced by L in the above expressions also for P_{cr}.

3) For fixed-fixed boundary conditions, $L_{eff}/L = 1$ per definition.

4) C_5 shall be calculated using the static soil stiffness in the L_{eff}/L calculation.

6.7.9 The L_{eff}/L term used above accounts for the effective span length in order to consider the span as fully fixed. This ratio decreases as the L/D_s ratio and soil stiffness increase.

The L_{eff}/L term is given by (for reference see Hobbs, 1986):

$$\frac{L_{eff}}{L} = \begin{cases} \dfrac{4.73}{-0.066\beta^2 + 1.02\beta + 0.63} & \text{for } \beta \geq 2.7 \\ \dfrac{4.73}{0.036\beta^2 + 0.61\beta + 1.0} & \text{for } \beta < 2.7 \end{cases}$$

$$\beta = \log_{10}\left(\frac{K\cdot L^4}{(1+CSF)EI}\right)$$

where K is the relevant soil stiffness (vertical or horizontal, static or dynamic).

6.7.10 The boundary coefficients in Table 6-1 based on the effective span length are found appropriate for fatigue assessment (FLS) under the assumption of small displacements and an isolated, single span on seabed.

For the check of maximum bending moments (ULS) due to direct wave loading, the pinned-pinned boundary condition may be applied in combination with the apparent span length (not the effective span length).

Guidance note:

The bending moment due to static deformations may be calculated by use of the boundary coefficients in Table 6-1 or alternative FE analysis applying long-term (static) soil stiffness.

---e-n-d---of---G-u-i-d-a-n-c-e---n-o-t-e---

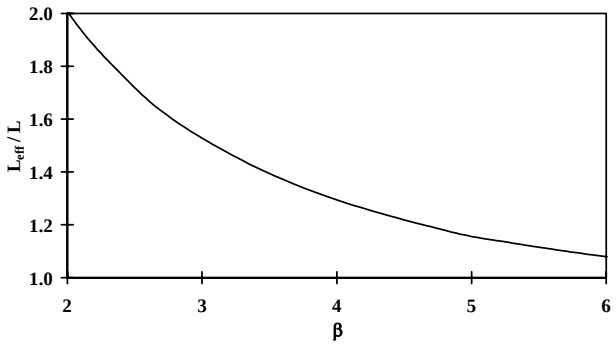

Figure 6-1
Effective span length as a function of β

6.8 Approximate response quantities for higher order modes of isolated single spans

6.8.1 For single spans (not multi-spans) in multi-mode vibrations, the approximate response quantities can be conservatively estimated based on Table 6-2.

Table 6-2 Approximate conservative higher order mode response quantities

Response	*2nd mode*	*3rd mode*	*4th mode*
Frequency 1)	2.7 f_1	5.4 f_1	8.1 f_1
Unit Stress amplitude	3.1 A_1	6.2 A_1	9.3 A_1

1) The fundamental frequency, f_1, shall be calculated without the sagging term. The critical force, P_{cr}, shall consider the frequency mode, i.e. the buckling length shall reflect the mode number.

Note that the sagging term should be excluded from the f_1 estimate for these higher order modes.

6.8.2 This approach is intended to be conservative, since the unit stress amplitudes given for 2nd, 3rd and 4th mode correspond to maximum values of the unit stress amplitudes, which do not occur at the same location of the span.

6.8.3 The approximate conservative response quantities for long spans in multimode are intended for screening purposes only.

6.9 Added mass

6.9.1 The added mass may be considered as:

$$C_a(e/D) = C_M\left(\alpha = 0;\ KC \downarrow 0;\ e/D\right) - 1$$

The ↓ symbolise KC approaching 0. Note that the effects of pipe roughness and trench are not accounted for.

According to Sec.5.4.9, C_a becomes:

$$C_a = \begin{cases} 0.68 + \dfrac{1.6}{(1 + 5\cdot(e/D))} & \text{for} \quad e/D < 0.8 \\ 1 & \text{for} \quad e/D \geq 0.8 \end{cases}$$

where e/D is the span gap ratio. This expression applies for both smooth and rough pipe surfaces.

6.9.2 The added mass coefficient given here is for calculation of still water frequency. The added mass coefficient in 4.5 is for modifying cross-flow response frequency and fatigue calculation only.

7. Pipe-soil Interaction

7.1 General

7.1.1 The soil is to be classified as cohesive (clays) or cohesionless (sands). As basis for the evaluations of the pipe-soil interaction the following basic soil parameters are relevant:

— type of soil
— in-situ stress conditions
— shear strength parameters for drained or undrained condition including remoulded shear strength for clays
— soil moduli and damping coefficients as function of cyclic shear strain
— soil settlement parameters
— general soil data as submerged unit weight, void ratio, water content and plasticity limits.

7.1.2 If the approximate soil stiffness expressions in 7.4 are to be used, then the following specific parameters are relevant:

— submerged unit weight of soil, γ_{soil}'
— Poisson's ratio, ν
— void ratio, e_s
— angle of friction, cohesionless soils, φ_s
— undrained shear strength, cohesive soils, s_u
— over-consolidation ratio, OCR
— plasticity index, cohesive soils, i_p.

The plasticity index i_p is a standard geotechnical parameter whose value is usually specified in the soil reports for the pipeline route. The plasticity index influences the dynamic spring stiffness given in 7.4.

7.1.3 The parameters listed above should preferably be obtained by means of geotechnical tests on undisturbed soil samples and be representative for the particular geographical location of the pipeline. In lieu of detailed information, the values given in Table 7-1 and Table 7-2 may be used as a guide in early phases of design.

Table 7-1 Typical geotechnical parameters for sand

Soil type	φ_s	γ_{soil}' *[kN/m³]*	ν	e_s
Loose	28 – 30°	8.5 – 11.0	0.35	0.7 – 0.9
Medium	30 – 36°	9.0 – 12.5	0.35	0.5 – 0.8
Dense	36 – 41°	10.0 – 13.5	0.35	0.4 – 0.6

Table 7-2 Typical geotechnical parameters for clay

Soil type	s_u *[kN/m²]*	γ_{soil}' *[kN/m³]*	ν	e_s
Very soft	< 12.5	4 – 7	0.45	1.0 – 3.0
Soft	12.5 – 25	5 – 8	0.45	0.8 – 2.5
Firm	25 – 50	6 – 11	0.45	0.5 – 2.0
Stiff	50 – 100	7 – 12	0.45	0.4 – 1.7
Very stiff	100 – 200	10 – 13	0.45	0.3 – 0.9
Hard	> 200	10 – 13	0.45	0.3 – 0.9

7.1.4 Uncertainties in the soil data should be considered, e.g. through sensitivity analysis. These uncertainties may arise from variations in the soil conditions along the pipeline route and difficulties in determining reliable in-situ soil characteristics of the upper soil layer, which is the soil of most importance for the pipeline. Soil data down to a depth equal to about 0.5-1.0 times the pipe diameter is most important to consider in this context. Since in general low strength of the soil is beneficial, leading to larger penetration, reduction in span length and higher lateral resistance, design should normally be based on high estimates of soil strength. If final acceptance of the pipeline is based on as-installed surveys e.g. to take account for un-

predictable installation effects, the available soil resistance should be evaluated based on low estimates of soil strength.

7.2 Modelling of pipe-soil interaction

7.2.1 The pipe-soil interaction is important in the evaluation of the static equilibrium configuration and the dynamic response of a free spanning pipeline. The following functional requirements apply for the modelling of soil resistance:

— The Seabed topography along the pipeline route must be represented.
— The modelling of soil resistance must account for non-linear contact forces vertical to the pipeline, e.g. lift off.
— The modelling of soil resistance must account for sliding in the axial direction. For force models this also applies in the lateral direction.
— Appropriate (different) short- and long-term characteristics for stiffness and damping shall be applied, i.e. static and dynamic stiffness and damping.

7.2.2 The seabed topography may be defined by a vertical profile along the pipeline route. The spacing of the data points characterising the profile should be related to the actual roughness of the seabed.

7.2.3 The axial and lateral frictional coefficients between the pipe and the seabed shall reflect the actual seabed condition, the roughness, the pipe, and the passive soil resistance.

7.2.4 The axial and lateral resistance is not always of a pure frictional type. Rapid changes in vertical stresses are (in low-permeable soil) reacted by pore water and not by a change in effective contact stresses between the soil and the pipe. In addition, the lateral resistance will have a contribution due to the penetration of the pipe into the soil, which needs be accounted for.

7.2.5 For sands with low content of fines, the frictional component of the axial and lateral resistance is proportional to the vertical force at any time. For clays, the resistance is proportional to the undrained shear strength.

7.2.6 The soil stiffness for vertical loading should be evaluated differently for static and dynamic analyses. The static soil response will be governed mainly by the maximum reaction, including some cyclic effects. Dynamic stiffness will be characterised mainly by the unloading/re-loading situation.

7.3 Soil damping

7.3.1 If no detailed assessment according to Appendix D is carried out, the modal soil damping ratio, ζ_{soil}, may be taken from Table 7-3 or Table 7-4. Interpolation is allowed.

Table 7-3 Modal soil damping ratios (in %) for sand

Sand type	*Horizontal (in-line) direction L/D*			*Vertical (cross-flow) direction L/D*		
	< 40	*100*	*> 160*	*< 40*	*100*	*> 160*
Loose	3.0	2.0	1.0	2.0	1.4	0.8
Medium	1.5	1.5	1.5	1.2	1.0	0.8
Dense	1.5	1.5	1.5	1.2	1.0	0.8

Note that the sand type is identified by the value of the friction angle φ_s (Table 7-1), and the clay type is identified by the value of the undrained shear strength s_u (Table 7-2).

For pipes supported by rock, values for the modal soil damping ratios may be taken as for dense sand.

Table 7-4 Modal soil damping ratios (in %) for clay

Clay type	*Horizontal (in-line) direction L/D*			*Vertical (cross-flow) direction L/D*		
	< 40	*100*	*> 160*	*< 40*	*100*	*> 160*
Very soft - Soft	4.0	2.0	1.0	3.0	2.0	1.0
Firm – Stiff	2.0	1.4	0.8	1.2	1.0	0.8
Very stiff - Hard	1.4	1.0	0.6	0.7	0.6	0.5

In addition to the modal soil damping ratios given in Tables 7-3 and 7-4, there will be structural damping, which in general is about 0.5%, but which may be as large as 1-2% when the pipe is designed with concrete coating.

7.4 Penetration and soil stiffness

7.4.1 The following expressions may be used for the static vertical soil reaction per unit length as a function of the vertical penetration, v:

Sand:

$$R_v = \gamma_{soil}' B(N_q v_{eff} + 0.5 N_\gamma B)$$

where the effective penetration, v_{eff}, is the larger of $(v - D/4)$ and 0, thereby accounting for the embedment effect of the pipe in a simplified manner.

Clay with constant undrained shear strength, s_u, with depth:

$$R_v = N_c s_u B + A_p \cdot \gamma_{soil}'$$

Clay with linear undrained shear strength, s_u, with depth:

$$R_v = B \cdot F \cdot (N_c s_{u0} + 0.25 \cdot kB) + A_p \cdot \gamma_{soil}'$$

Symbols used:

B Contact width for pipe-soil load transfer:

$$= \begin{cases} 2\sqrt{(D - v)v} & \text{for } v \le 0.5D \\ D & \text{for } v > 0.5D \end{cases}$$

D Outer pipe diameter (including any coating)

γ_{soil}' Submerged unit weight of soil.

s_u Undrained shear strength

s_{u0} Undrained shear strength at seabed

F Correction factor to account for increasing shear strength with depth. Also depending on pipe surface roughness, cf. Figure 7-2. Rough pipe surface refers to full mobilisation of soil shear strength, whereas smooth pipe surface corresponds to zero surface shear. For pipe surface roughness between rough and smooth, the value of F may be interpolated between the values in Figure 7-2 for rough and smooth surfaces.

k Depth gradient of undrained shear strength

A_p Cross-sectional area of penetrated part of pipe

The expressions for R_V are based on bearing capacity formulas for ideal 2-D strip foundations. Note that if these formulas are used to predict the expected penetration v for a given contact force R_V, they may lead to underestimation of the true penetration due to effects of the pipe laying process and erosion as well as possible 3-D effects on the shoulders near the free span.

The contact force per unit length experienced during pipe laying may significantly exceed the static contact force due to the weight of the pipe (typically by a factor of 1.3 - 2.0). Also a simultaneously occurring horizontal force will increase the penetration. This may be accounted for by using bearing capacity formulae adjusted for inclined loading, as given in DNV Classification Notes No. 30.4. Repeated horizontal oscillation will tend to further increase the penetration. If the horizontal loading is motion-controlled rather than force-controlled, such effects could be evaluated from empirical results. The bearing capacity factors N_c, N_q and N_g versus the internal friction angle φ_s may be calculated from the following formulas:

$$N_q = \exp(\pi \tan \varphi_s) \tan^2(45 + \frac{\varphi_s}{2})$$

$$N_c = 5.14$$

$$N_\gamma = 1.5(N_q - 1) \tan \varphi_s$$

For clayey soils the friction angle is set equal to 0°.

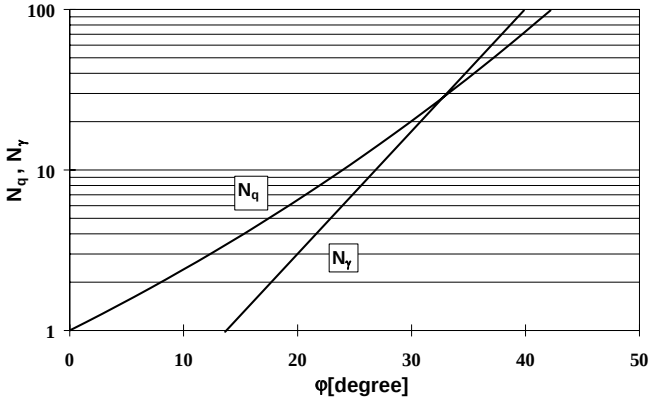

Figure 7-1
Bearing capacity factors Nc, Nq and Nγ versus the internal friction angle φ_s

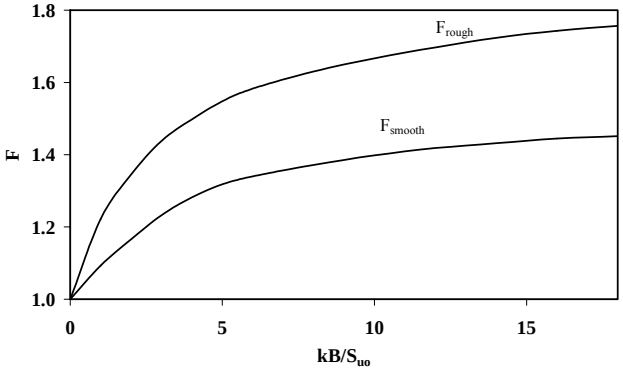

Figure 7-2
Correction factor F for rough and smooth pipe-soil interface

7.4.2 The available capacity for transfer of axial loads between pipe and soil should be considered.

Axial frictional stresses may exist between pipe and soil, e.g. formed by residual stresses from the pipelay. When such axial stresses are present, they may prevail over long distances far back from the point of separation between pipe and soil on the shoulder of the free span.

The axial friction will be limited by the available surface friction. The available surface friction, in turn, will be limited by the undrained shear strength for clays and by the frictional coefficient for sands. In areas with lateral movements of the pipe, typically on the shoulders near the free span, the available surface friction has to be shared between axial and lateral stresses. This further limitation on the available axial friction during lateral movements may lead to redistribution of axial stresses away from the free span.

7.4.3 The static vertical stiffness $K_{V,S}$ is a secant stiffness representative for penetration conditions such as during installation and erosion and during development of free spans.

The static vertical stiffness $K_{V,S}$ is defined as $K_{V,S} = R_V/v$, where R_V is the static vertical soil reaction per unit length of pipe and v is the vertical penetration of the pipe required to mobilise this reaction. Unless effects of pipelay and erosion and 3-D shoulder effects are significant, the 2-D approach outlined in 7.4.1 can be used to predict v. Otherwise, or when no detailed information is available, the static stiffness value may be taken according to Table 7-5 for sand and Table 7-6 for clay.

7.4.4 The vertical dynamic stiffness K_V is defined as $K_V = \Delta F_V/\Delta\delta_V$, where ΔF_V is the dynamic vertical force between pipe and soil per unit length of pipe, and $\Delta\delta_V$ is the associated vertical displacement of the pipe, measured relative to the static position of the pipe.

7.4.5 The lateral (horizontal) dynamic stiffness K_L is defined as $K_L = \Delta F_L/\Delta\delta_L$, where ΔF_L is the dynamic horizontal force between pipe and soil per unit length of pipe, and $\Delta\delta_L$ is the associated horizontal displacement of the pipe.

7.4.6 For determination of K_V, the following expression may be applied:

$$K_v = \frac{0.88 \cdot G}{1 - \nu}$$

which is based on elastic half space theory for a rectangular foundation under assumption of a pipe length that equals 10 times the contact width between pipe and soil. Poisson's ratio ν is given in Table 7-1 and Table 7-2.

7.4.7 For determination of K_L, the following expression may be applied:

$$K_L = 0.76 \cdot G \cdot (1 + \nu)$$

which is based on elastic half space theory for a rectangular foundation under assumption of a pipe length that equals 10 times the contact width between pipe and soil. Poisson's ratio ν is given in Table 7-1 and Table 7-2.

The shear modulus G may be calculated according to the approach specified in D.2.1.

7.4.8 The mean effective stress, σ_s, in the soil at the span supports may be calculated from the stress conditions at a representative depth below the pipe. The representative depth may be assumed equal to the contact width B, which is given in 7.4.1. The following formula may then be applied:

$$\sigma_s = \frac{1}{2}(1 + K_0) B \gamma_{soil}' + \frac{q}{3B}(1 + \frac{L}{2L_{sh}})$$

where

K_0	Coefficient of earth pressure at rest. Usually $K_0 = 0.5$, however, values of K_0 in excess of 1.0 may exist for clays with large over-consolidation ratios
γ_{soil}'	Submerged unit weight soil (kN/m^3)
q	Submerged weight of pipe per unit length of pipe (kN/m)
L_{sh}	Span support length on one shoulder (for transfer of one-half the weight of the free span)
L	Span length

Note that for pipes on clay, the clay might not be consolidated for the weight of the pipe in the temporary phase immediately after pipelay. For calculations for a pipe on clay in this phase, the formula for σ_s reduces to

$$\sigma_S = \frac{1}{2}(1+K_0)B\gamma_{soil}'$$

The span support length L_{sh}, which is the contact length between pipe and soil on one shoulder, depends on the span length, the soil stiffness on the shoulders, the soil type, the shoulder geometry, and the submerged weight and stiffness of the pipe.

7.4.9 If there are indications that the values for K_V and K_L should be different from those produced by the procedure in 7.4.6 - 7.4.8, then the ratio between the assumed pipe length on the shoulder and the contact width may be adjusted from the adopted value of 10. Calculation of the mean effective stress σ_s from the stress conditions at a different representative depth below the pipe than B may also be considered. Note that, in this context, it is acceptable to distinguish between representative depths for calculation of K_V and for calculation of K_L.

7.4.10 When the topographical conditions are not complex, when the soils are non-stratified and homogeneous, and when no detailed analysis is carried out for determination of K_V and K_L according to the approach specified in 7.4.6 - 7.4.8, the values of these stiffness in units of kN/m/m may be calculated in simplified manner as:

$$K_V = \frac{C_V}{1-\nu}\left(\frac{2}{3}\frac{\rho_s}{\rho}+\frac{1}{3}\right)\sqrt{D}$$

$$K_L = C_L(1+\nu)\left(\frac{2}{3}\frac{\rho_s}{\rho}+\frac{1}{3}\right)\sqrt{D}$$

in which the pipe diameter D is in units of metres and the coefficients C_V and C_L are taken according to Table 7-5 and Table 7-6. The soil type, which is used as entry to these tables, is identified by the value of the friction angle φ_s for sand (Table 7-1) and by the value of the undrained shear strength s_u for clay (Table 7-2). It must be assessed whether the soil conditions are drained or undrained. For undrained conditions, Poisson's ratio is $\nu = 0.5$, whereas for drained conditions Poisson's ratio is $\nu < 0.5$. The expressions are valid for $1.2 < \rho_s/\rho < 2.0$.

Table 7-5 Dynamic stiffness factor and static stiffness for pipe-soil interaction in sand

Sand type	C_V *(kN/m$^{5/2}$)*	C_L *(kN/m$^{5/2}$)*	$K_{V,S}$ *(kN/m/m)*
Loose	10500	9000	250
Medium	14500	12500	530
Dense	21000	18000	1350

Table 7-6 Dynamic stiffness factor and static stiffness for pipe-soil interaction in clay with OCR = 1

Clay type	C_V *(kN/m$^{5/2}$)*	C_L *(kN/m$^{5/2}$)*	$K_{V,S}$ *(kN/m/m)*
Very soft	600	500	50-100
Soft	1400	1200	160-260
Firm	3000	2600	500-800
Stiff	4500	3900	1000-1600
Very stiff	11000	9500	2000-3000
Hard	12000	10500	2600-4200

7.4.11 For free spans supported by sand, the lateral dynamic stiffness K_L should be calculated under an assumption of loose sand properties in order to properly account for effects of complex soil mobility, including erosion and self burial.

7.4.12 For extreme conditions, which can be assumed to cause large deformations on the shoulders, a smaller spring stiffness than that associated with small-strain conditions applies.

The situation that lateral drag loads from waves are large enough that the pipe not only oscillates but literally slides on the shoulders, involving large lateral displacements, calls for a model which can represent the involved nonlinear force-displacement relationship between pipe and soil properly. In this clause, a bilinear model for the force-displacement curve for this situation is given. This model covers the transition from small-strain conditions towards extreme displacement conditions. The model has been calibrated to data from a few pipelines only, so caution should be exercised whenever the model is a candidate for application. Note that other relevant methods may also be applied. See Appendix D for a general description of soil-pipeline interaction.

A bilinear model, which may be applied at span supports on sand and clay, reads:

$$F_L = \begin{cases} k_1 \cdot y & \text{for } F_L < \mu_L F_V \\ \mu_L F_V + k_2 \cdot (y - \frac{\mu_L F_V}{k_1}) & \text{for } \mu_L F_V \le F_L < F_{L,max} \end{cases}$$

y	Lateral displacement of pipe on shoulder
F_L	Lateral force per unit length of pipe at displacement y
$F_{L,max}$	Maximum lateral resistance per unit length of pipe
F_V	Vertical contact force per unit length of pipe on shoulder
μ_L	Lateral friction coefficient
k_1	Equivalent secant stiffness up to mobilisation of full friction
k_2	Equivalent stiffness for deformations past mobilisation of full friction

Unless data indicate otherwise, $\mu_L = 0.6$ may be applied for span supports on sand and $\mu_L = 0.2$ for span supports on clay.

For supports on sand, the initial stiffness k_1 may be taken as equal to the lateral dynamic stiffness K_L for loose sand. For supports on clay, the initial stiffness k_1 may be taken as equal to the lateral dynamic stiffness K_L for the clay type in question.

The equivalent stiffness k_2 depends on the vertical penetration, v, of the pipe on the shoulder. For span supports on sand, values for k_2 are given in Table 7-7.

Table 7-7 Equivalent stiffness, k_2, for span supports on sand

v/D	*k_2 (kN/m/m)*
0.00	0
0.25	19
0.35	28
0.50	44
1.00	105

For span supports on clay, the equivalent stiffness k_2 can be calculated as

$$k_2 = 8.26 \cdot s_u \cdot \left(\frac{s_u}{D\gamma_{soil}}\right)^{-0.4} \cdot \left(\frac{v}{D}\right)^{1.3}$$

where

γ_{soil}'	Submerged unit weight of soil
γ_{water}	Unit weight of water (= 10 kN/m^3)
γ_{soil}	Total unit weight of soil (= γ_{soil}' + γ_{water})
v	Vertical pipe penetration at span shoulder

This stiffness corresponds to an assumed mobilisation of $F_{L,max}$ at an additional lateral displacement of D/2 beyond the mobilisation of the friction part of the resistance.

For span supports on sand, the maximum lateral resistance per unit length of pipe is

$$F_{L,max} = \mu_L F_V + 5.0 \cdot \gamma_{soil}' \cdot D^2 \cdot \left(\frac{v}{D}\right)^{1.25}$$

For span supports on clay, the maximum lateral resistance per unit length of pipe is

$$F_{L,max} = \mu_L F_V + 4.13 \cdot D \cdot s_u \cdot \left(\frac{s_u}{D\gamma_{soil}}\right)^{-0.4} \cdot \left(\frac{v}{D}\right)^{1.3}$$

For clay, the stiffness and resistance values of the bilinear model are partly documented by Verley and Lund (1995). Caution should be exercised not to use the bilinear model outside the limits specified in Verley and Lund (1995).

7.4.13 The axial dynamic soil stiffness is usually not important. However, when long free spans are considered, it is important to include an axial soil-support model with friction and stiffness. If no information is available about the axial dynamic soil stiffness, it may be taken as equal to the lateral dynamic soil stiffness K_L as described above.

7.5 Artificial supports

7.5.1 Gravel sleepers can be modelled by modifying the seabed profile, considering the rock dump support shape and applying appropriate stiffness and damping characteristics.

7.5.2 The purpose of mechanical supports is generally to impose locally a pipeline configuration in the vertical and/or transverse directions. Such supports can be modelled by concentrated springs having a defined stiffness, taking into account the soil deformation beneath the support and disregarding the damping effect.

8. References

Andersen, K.H. (2004) "Cyclic clay data for foundation design of structures subjected to wave loading." International Conference on Cyclic Behaviour of Soils and Liquefaction Phenomena, Bochum, Germany 2004. Proceedings, pp. 371-387.

Blevins, R.D., "Flow-Induced Vibrations", Krieger Publishing Company, Florida, 1994

Bruschi, R. & Vitali, L., "Large-Amplitude Oscillations of Geometrically Non-linear Elastic Beams Subjected to Hydrodynamic Excitation", JOMAE, Vol. 113, May, 1991.

Chezhian, M., Mørk, K.J., Fyrileiv, O., Nielsen, F.G., Søreide, T. 'Assessment of Deepwater Multi-Spanning Pipelines – Ormen Lange Experience',15th Deep Offshore Technology (International Conference & Exhibition), - Marseille, France, November 19-21, 2003.

DNV Offshore Standard OS-F101, "Submarine Pipeline Systems".

DNV Offshore Standard OS-F201, "Dynamic Risers".

DNV Recommended Practice DNV-RP-F204 "Riser Fatigue".

DNV Recommended Practice RP-C203, "Fatigue Strength Analysis of Offshore Steel Structures".

DNV Recommended Practice RP-E305, "On-bottom Stability Design of Submarine Pipelines".

Fyrileiv, O., Mørk, K.J. & Rongved, K. "TOGI Pipeline – Assessment of Non-stationary Free Spans", OMAE'00, New Orleans, USA, February 14-17, 2000.

Fyrileiv, O. and Mørk, K. , "Structural Response of Pipeline Free Spans based on Beam Theory", Proc. of 22nd International Conference on Offshore Mechanical and Arctic Engineering, OMAE 2002, Oslo, Norway, June 23-28, 2002.

Fyrileiv, O., Chezhian, M., Mørk, K.J., Arnesen, K., Nielsen, F.G., Søreide, T. 'New Free Span Design Procedure for Deepwater Pipelines',16th Deep Offshore Technology (International Conference & Exhibition), - New Orleans, USA, 2004.

Fyrileiv, O., Chezhian, M. and Mørk, K., "Experiences Using DNV-RP-F105 in Assessment of Free Spanning Pipelines", Proc. of 24rd International Conference on Offshore Mechanical and Arctic Engineering, OMAE 2005 Halkidiki, Greece, June 2005.

Hagen, Ø., Mørk, K.J., Nielsen, F.G., Søreide, T. 'Evaluation of Free Spanning Design in a Risk Based Perspective', 22nd International conference on Offshore Mechanics and Arctic Engineering, (OMAE2003-37419), Cancun, Mexico, June 8-13, 2003.

Hansen, E.A., Bryndum, M., Mørk, K.J., Verley, R., Sortland, L. & Nes, H.,"Vibrations of Free Spanning Pipeline Located in the Vicinity of a Trench", OMAE'01-4016, Rio de Janeiro, Brazil, June 3-8, 2001.

Hardin, B.O., "The nature of stress-strain behavior for soils," Proceedings, ASCE Geotech. Engrg. Div. Specialty Conf. on Earthquake Engineering and Soil Dynamics, Vol. 1, pp. 3-90, 1978.

Hobbs, R.E:, "Influence of Structural Boundary Conditions on pipeline Free Span Dynamics", OMAE'86, 1986.

Larsen, C.M, & Koushan, K. "Emperical model for the analysis of vortex induces vibrations of free spanning pipelines", EURODYN 2005, ISBN 90 5966 033 1

Mørk, K.J., Vitali, L. & Verley, R., "The MULTISPAN Project: Design Guideline for Free Spanning Pipelines", Proc. of OMAE'97 conf., Yokohama, Japan, April 13-17, 1997.

Mørk, K.J. & Fyrileiv, O. "Fatigue Design According to the DNV Guideline for Free Spanning Pipelines", OPT'98, Oslo, Norway, February 23-24, 1998.

Mørk K.J., Fyrileiv, O., Verley, R., Bryndum, M. & Bruschi, R. "Introduction to the DNV Guideline for Free Spanning Pipelines", OMAE'98, Lisboa, July 6-9, 1998.

Mørk, K.J., Fyrileiv, O., Nes, H. & Sortland, L. "A Strategy for Assessment of Non-Stationary Free Spans", ISOPE-99, Brest, France, May 30-June 4, 1999.

Mørk, K.J., Fyrileiv, O., Chezhian, M., Nielsen, F.G., Søreide, T. 'Assessment of VIV Induced Fatigue in Long Free Spanning Pipelines', 22nd International conference on Offshore Mechanics and Arctic Engineering, (OMAE2003-37124), Cancun, Mexico, June 8-13, 2003.

Nielsen, F.G., Kvarme, S.O. and Søreide, T. VIV response of long free spanning pipelines. 21st International conference on offshore mechanics and arctic engineering, (OMAE), Oslo, Norway, 2002.

Sumer B.M. and Fredsøe, J. "Hydrodynamics around Cylindrical Structures", Advanced Series on Ocean Engineering – Volume 12, World Scientific, London, 1997.

Tura, F., Dumitrescu, A., Bryndum, M. B. & Smed, P.F. "Guidelines for Free Spanning Pipelines: The GUDESP Project", OMAE'94, Volume V, pp 247-256, Houston, 1994.

Verley, R. and Lund, K.M., "A Soil Resistance Model for Pipelines placed on Clay Soils," Proceedings, OMAE1995, Vol. V, pp. 225-232, Copenhagen, Denmark, 1995.

APPENDIX A
MULTI-MODE RESPONSE

A.1 Applicability

A.1.1 In case several potential vibration modes can become active at a given flow velocity, the multi-mode response approach given in this section should be adopted.

A.1.2 Multi-spans should always be assessed with the multi-mode response approach.

A.1.3 This approach can be applied for both single spans and multispans. It can also be applied to compute the fatigue damage, when two or more modes are competing with each other, i.e. when the eigen frequencies are close.

A.1.4 The fundamental fatigue design approach and the principle of application of response models are similar to the principles given in Sec.4. The extension of the design methodology to the multi-mode response is covered in this section.

A.2 Computational approach

A.2.1 The in-line and cross-flow eigen frequencies and associated mode shapes need to be calculated by a FE analysis, by taking into account the span sag and appropriate boundary conditions at the span shoulder. It is assumed that all parameters that are typically required for a conventional free span analysis, such as geometric and material properties, the operational pressure and temperature, seabed characteristics are available. Proper sequence of loading / pressurising must be accounted for.

A.2.2 At a given flow velocity, the procedure given in A.3 to A.6 is applied. See also Figure A-1.

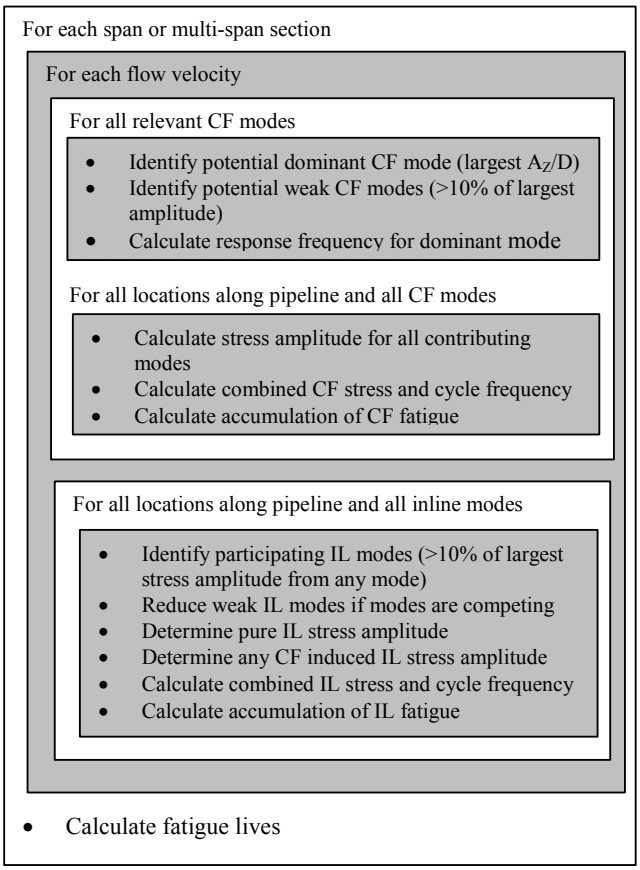

Figure A-1
Calculation flow chart for multi-mode response

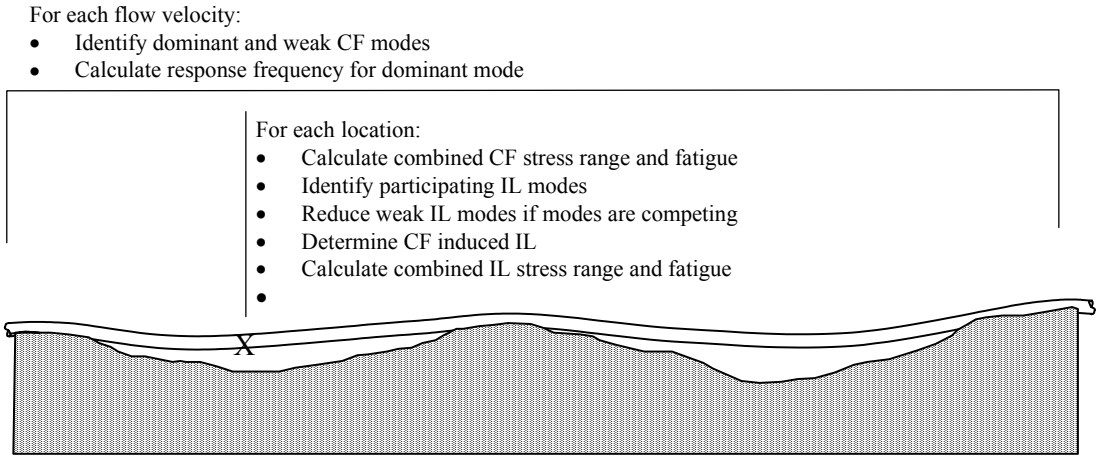

Figure A-2
Multi-span section with multi-mode response

A.2.3 The computational procedure is exemplified by considering 3 'contributing' cross-flow modes and for 4 'contributing' in-line modes. In most practical cases, this is considered sufficient to capture the underlying physics and provide accurate engineering estimates of the fatigue damage.

However, it is straight forward to extend this approach to more modes.

Guidance note:

The lower order modes (e.g. mode no. 1, 2, 3) are typical relevant for the operational phase, while higher order modes (e.g. mode no. 5, 6, 7) may be relevant for temporary conditions where the lower order modes may have passed the V_R range that causes vibrations to be excited (in-line VIV).

---e-n-d---of---G-u-i-d-a-n-c-e---n-o-t-e---

A.3 Cross-flow response

A.3.1 Only pure cross-flow response is considered, i.e. potential IL induced cross-flow response at $V_R \sim 2$ to 3 is neglected.

A.3.2 The 'contributing' cross-flow modes are defined later in A.3.3. In possible multi-span scenarios, the full length of the pipe section must be analysed to identify possible interaction between spans. The following approach should be applied to each section length of a multi-spanning pipeline or for the entire span length, in case of long single spans.

A.3.3 For each section length and flow velocity considered, the cross-flow mode with the largest A_Z/D value predicted from the response model at the given reduced velocity is defined as the dominant cross-flow mode. The contributing modes are defined as the modes for which the maximum A_Z/D in the span is at least 10% of the maximum A_Z/D of the dominant cross-flow mode. The other cross-flow modes, which are contributing but do not dominate, are referred to as the "weak" cross-flow modes.

A.3.4 The maximum stress range induced by the dominant cross-flow mode *i*, is assessed using the response model:

$$S_{i,CF}(x) = 2 \cdot A_{i,CF}(x) \cdot (A_{Z_i} / D) \cdot R_k \cdot \gamma_s$$

Here $A_{i,CF}(x)$ is the unit diameter stress amplitude of the cross-flow mode *i* and the A_Z/D is the non-dimensional response amplitude computed based on the response model, see 4.4.3 for more details. The position at which the stress is calculated, along the length of the free span is given in terms of the span co-ordinate, *x*.

A.3.5 The stress range induced by the weak cross-flow modes is assessed by the following expression:

$$S_{i,CF}(x) = 2 \cdot 0.5 \cdot A_{i,CF}(x) \cdot (A_{Z_i} / D) \cdot R_k \cdot \gamma_s$$

A.3.6 The combined cross-flow induced stress is given as the 'square root of the sum of squares' (SRSS) value:

$$S_{comb,CF}(x) = \sqrt{\sum_{i=1}^{n} \left(S_{i,CF}(x)\right)^2}$$

where 'n' is the number of cross-flow modes present at a given velocity.

A.3.7 The cycle counting frequency, $f_{cyc,CF}(x)$, for this combined cross-flow induced stress, is taken as the weighted SRSS frequency:

$$f_{cyc,CF}(x) = \sqrt{\sum_{i=1}^{n} \left(f_{i,CF} \frac{S_{i,CF}(x)}{S_{comb,CF}(x)} \right)^2}$$

where $f_{i,CF}$ is taken as cross-flow response frequency for the dominant mode and as the still water eigen frequency for the weak cross-flow modes.

$f_{i,CF} = f_{i,CF-RES}$ for the dominant cross-flow mode

$f_{i,CFi} = f_{i,CF}$ for the weak cross-flow modes (still water frequency)

A.4 In-line response

A.4.1 A larger number of active modes is typical for the in-line response computation compared to cross-flow. The effect of cross-flow induced IL motion, also needs to be considered when relevant.

A.4.2 The procedure is explained for four 'contributing' in-line modes, which may be potentially activated.

A.4.3 These four contributing modes are not necessarily the first four modes, but rather the first four contributing (participating) modes as described later in this section.

A.5 Pure in-line VIV

A.5.1 When two modes are very close in frequency, they are both strong candidate for responding at the same current velocities, i.e. lock-in ranges overlap. The result being that one mode only obtains full response, i.e. a response following the response models given in Sec.4. The other modes have a reduced response.

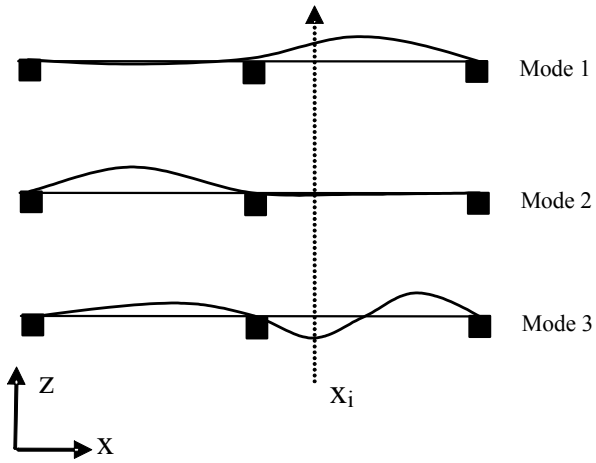

Figure A-3
Determination of active in-line modes

A.5.2 An example case with in-line modes for a multi-spanning pipeline is shown in Figure A-3. The first step is to determine the active modes at each location along the length of the free span (i.e. at each x coordinate, denoted as x_i in Figure A-3).

A.5.3 At a given location x_i, the relative importance of the "response stress" is assessed for all modes. The n^{th} mode is ignored if the response stress of n^{th} mode at $x_i < 10\%$ of the largest response stress of all other potential modes at x_i. By eliminating these inconsequential modes, the final list of actively participating modes is determined.

Guidance note:

For the example case shown in Figure A-3, mode 1 and mode 3 are short listed as the actively participating modes and mode 2 is ignored at x_i.

---e-n-d---of---G-u-i-d-a-n-c-e---n-o-t-e---

A.5.4 The actively participating modes are renumbered, excluding the inconsequential modes.

Guidance note:

For the example case shown in Figure A-3, the renumbering is done as follows.

Old number	*Renumbered (as consecutive modes)*
Mode 1	Mode 1
Mode 2 (ignored for the given location and for a given current velocity, U_i)	-
Mode 3	Mode 2
Mode 4	Mode 3

---e-n-d---of---G-u-i-d-a-n-c-e---n-o-t-e---

A.5.5 Two adjacent modes can either compete with each other, when their frequencies are close or they can act as independent modes, when their frequencies are widely separated.

A.5.6 For computational purposes, the renumbered mode system should be used, when two adjacent mode numbers need to be checked.

A.5.7 Two adjacent modes are competing, if the ratio of their frequencies is lower than 2, i.e.

$$\frac{f_{n+1}}{f_n} < 2$$

where f_n is the eigen frequency of the n^{th} mode number.

A.5.8 When the modes compete, only one of the modes is assumed to respond (i.e. is permitted to respond) with the full A/D as given in Sec.4. This mode is referred to as the dominant in-line mode. The remaining actively participating modes will be subject to a reduction in the permissible amplitude and the response of these weak (non-dominant) in-line modes may be reduced by a factor of 0.5.

A.5.9 Every adjacent mode combination needs to be checked, to find out which ones will compete and which modes will win the competition. This implies the following combinations needs to be checked:

— Mode 1 – Mode 2
— Mode 2 – Mode 3
— Mode 3 – Mode 4

A.5.10 Evaluate the stress at the given location x_i, for all the actively participating modes. The competing mode reduction factor, α_j, is multiplied to the stresses associated with each of the mode shapes, based on the following rules:

Non-competing mode combinations

— For non-competing mode combinations, the α_j, is always 1, i.e. there is no stress reduction.

Competing mode combinations

— The mode associated with the largest stress (i.e. dominant mode) within each competing mode combination gets an α_j of 1.
— The weak mode within each competing mode combination gets an α_j of 0.5.
— The competing modes reduction factor, α_j, should be multiplied to the stresses, for each mode combination checked. This implies that for some mode numbers, it can be applied more than once on the same mode number.

Guidance note:

Consider an example case, where

— Mode 1 and Mode 2 are competing and assume Mode 1 is the dominant mode in this competition. This implies Mode 1 get an α_j of 1 and Mode 2 gets an α_j of 0.5.
— Mode 2 and Mode 3 are competing and assume Mode 2 is the dominant mode in this competition. This implies Mode 2 get an α_j of 1 and Mode 3 gets an α_j of 0.5.
— Mode 3 and Mode 4 are competing and assume Mode 4 is the dominant mode in this competition. This implies Mode 4 get an α_j of 1 and Mode 3 gets an α_j of 0.5.

This will effectively imply that:

— Mode 1 get an α_j of 1
— Mode 2 gets an α_j of 0.5
— Mode 3 gets an α_j of 0.25 (= 0.5 · 0.5)
— Mode 4 gets an α_j of 1.0

Since Mode 3 is competing with Mode 2 as well as Mode 4, this further reduction (0.25) is justified.

---e-n-d---of---G-u-i-d-a-n-c-e---n-o-t-e---

A.5.11 The pure in-line VIV stress range $S_{j,IL}$ (x) is written as:

$$S_{j,IL}(x) = 2 \cdot \alpha_j \cdot A_{j,IL}(x) \cdot (A_Y / D) \cdot \psi_{\alpha,IL} \cdot \gamma$$

where the effect of the reduction factor for competing modes, α_j, has been included. For more details, see Sec.4.3.3.

Guidance note:

Applying no reduction factor for competing modes (α_j = 1.0) is conservative.

---e-n-d---of---G-u-i-d-a-n-c-e---n-o-t-e---

A.6 Cross-flow induced in-line VIV

A.6.1 It is assumed that only the dominant cross-flow mode can potentially contribute to the cross-flow induced in-line motion.

A.6.2 The in-line mode with its eigen frequency closest to twice the dominant cross-flow response frequency is chosen as the candidate for the cross-flow induced in-line:

$$\min\left(\left| f_{j,IL} - 2 \cdot f_{i,CF-RES} \right|\right)$$

where j = 1,2,….,2n and i denotes the dominating cross-flow mode.

A.6.3 The in-line stress range corresponding to a figure **8** or half-moon motion, $S_{IL-CF-DOM,j}(x)$, i.e., the dominant cross-flow mode induces the j^{th} in-line mode and the corresponding in-line stress can be written as:

$$S_{j,IL-CF}(x) = 2 \cdot 0.4 \cdot A_{j,IL}(x) \cdot (A_{Z_{DOM}} / D) \cdot R_k \cdot \gamma$$

A.6.4 The stress for the in-line mode that is potentially oscillated by cross-flow induced in-line motion, is taken as:

$$S_{j,IL}(x) = \max\left(S_{j,IL}(x), S_{j,IL-CF}(x)\right)$$

A.6.5 The combined in-line stress is given as the 'square root of the sum of squares' (SRSS) value:

$$S_{comb,IL}(x) = \sqrt{\sum_{j=1}^{2n} \left(S_{j,IL}(x)\right)^2}$$

A.6.6 The cycle counting frequency for the in-line modes is based on the following principles:

— for pure in-line modes, the cycle counting frequency is the still water eigen frequency of the in-line mode
— for the cross-flow induced in-line mode, the cycle counting frequency is taken as twice the cross-flow response frequency of the dominant cross-flow mode, i.e. $2 \cdot f_{i,CF-RES}$.

A.6.7 The combined stress and associated cycle counting frequency, using SRSS approach, is given by

$$f_{cyc,IL}(x) = \sqrt{\sum_{j=1}^{2n} \left(f_{j,IL} \frac{S_{j,IL}(x)}{S_{comb,IL}(x)} \right)^2}$$

APPENDIX B
VIV MITIGATION

B.1 VIV mitigation methods

B.1.1 The most commonly used vortex suppression devices are helical strakes. Their function is to trigger separation in order to decrease the vortex shedding correlation along the riser. They increase the cost of the pipeline, and they will complicate handling during installation. The in-line drag coefficient is increased by introducing strakes.

B.1.2 The important parameters for the strake design are the height and pitch of the helical strakes for a given pipeline diameter. The overall performance characteristics of a given strake design will vary with the current velocities.

B.1.3 The effectiveness of VIV suppression devices, such as VIV strakes needs to be qualified. It is recommended that an independent verification of the effectiveness of VIV suppression devices is performed by a competent verification body.

B.1.4 Qualification process will typically include the following, for a given strake design:

— model test results with and without strakes
— effect of hydrodynamic scaling
— range of current velocities and associated efficiency
— durability and impact assessments
— effect of marine growth
— effect of surface finish.

B.1.5 More detailed information is given in DNV-RP-F204 with respect to qualification of VIV strakes.

B.2 Span rectification methods

B.2.1 Reference is made to Sec.9 of DNV-OS-F101 for span rectification procedures and methods.

B.2.2 Survey, follow-up and documentation requirements should follow the principles given in Sec.9 of DNV-OS-F101.

APPENDIX C
VIV IN OTHER OFFSHORE APPLICATIONS

C.1 Main application scope

C.1.1 The primary focus and the main application scope of this RP is free spanning subsea pipelines as described in Sec.1.3.

C.1.2 The fundamental principles given in this RP may also be applied and extended to other offshore elements such as cylindrical structural elements of the jackets, risers from fixed platforms etc., at the designer's discretion. The limitations that apply are discussed in this section.

C.2 Riser VIV

C.2.1 Important differences with respect to the riser VIV, as compared to free spanning VIV are listed below:

— The circular particle flow due to waves.
— Risers will not experience the uniform currents over the span, as assumed in free span assessments.
— Typically for long risers, the higher order modes are excited.
— For long span lengths and/or when the flow is sheared, several modes may be excited simultaneously. For such risers the tension will vary, and the response is dominated by loading (power input) in some parts of the riser while other parts are contributing to the damping of the system (power output). In such cases DNV-RP-F105 is not applicable.

C.2.2 For short riser span lengths, typical for steel risers supported by a jacket structure and when the current is uniform, the response models given in Sec.4 of this RP (DNV-RP-F105) can be applied. For short risers the lowest eigen modes are typically excited. In such cases DNV-RP-F105 will predict both in-line and cross-flow VIV provided that the natural frequencies are calculated based on relevant boundary conditions.

C.2.3 If no onset of VIV is allowed, the screening criterion may be applied.

C.2.4 Other subsea cylindrical structural components (e.g. braces, trusses, etc.) can also be evaluated, using this RP at the designers discretion and judgement. The following conditions should however, be carefully evaluated:

— uniform current assumption
— frequencies and mode shapes should be based on detailed FE analysis
— L/D ratio should be within the RP's design range
— location of the structural element (relevance of Wave-induced VIV, which is not covered by this RP).

C.2.5 For a detailed account of riser VIV and applicable methodologies, reference is made to the DNV-RP-F204 "Riser Fatigue".

APPENDIX D
DETAILED ASSESSMENT OF PIPE-SOIL INTERACTION

D.1 General

D.1.1 The pipe-soil interaction is complex and depends strongly on several parameters like the loading history, load rate and amplitude. In the following a detailed approach to establish important soil characteristics like stiffness and damping is given.

D.1.2 Wherever linear soil stiffness has to be defined for the eigen value analysis, the soil stiffness should be selected considering the actual soil resistance and the amplitude of the oscillations.

D.2 Soil stiffness

D.2.1 The soil stiffness may be evaluated from the shear modulus G of the soil. The shear modulus G, defined as a secant modulus, is a decreasing function of the shear strain amplitude γ_c in the soil. The shear modulus G_{max} at small strains may be calculated from the following expression

$$G_{\max} = 625 \cdot \frac{OCR^{k_s}}{0.3 + 0.7 e_s^{\,2}} \sqrt{\sigma_a \sigma_s}$$

where

σ_a	Atmospheric pressure (100 kPa)
σ_s	Mean effective stress in soil
OCR	Over consolidation ratio for clayey soils, to be set equal to 1.0 for sands
e_s	Void ratio
k_s	Coefficient, taken from Figure D -1

The expression for G_{max} is originally formulated by Hardin (1978) and is based on experimental results for a broad range of soil types.

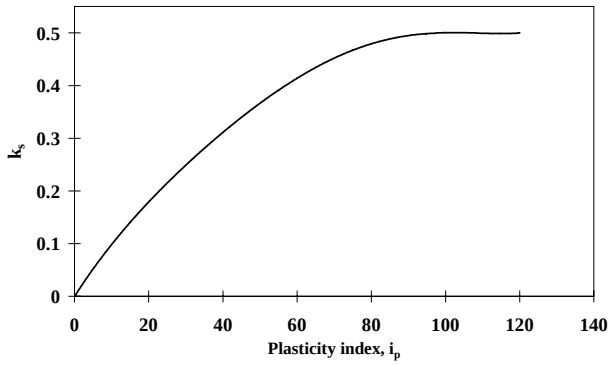

Figure D-1
k_s versus plasticity index, I_p (%)

For clays, the small-strain shear modulus G_{max} may alternatively be calculated from the undrained shear strength s_u in the following manner, as an approximation to laboratory test data (e.g. Andersen 2004):

$$\frac{G_{\max}}{s_u} = \frac{300}{I_p}$$

where I_p denotes the plasticity index (in absolute numbers).

The relation between the secant shear modulus G and the cyclic shear strain amplitude γ_c is typically expressed as a curve of G/G_{max} versus γ_c. Unless data indicate otherwise, the curves given in Figure D-2 for various plasticity indexes I_p may be used to calculate G/G_{max}. The curve for $I_p = 0$ applies to saturated cohesionless soils such as sand, whereas the curves for $I_p > 0$ applies to clays. The curves should be used with caution, since they represent the mean of data which exhibit a large scatter.

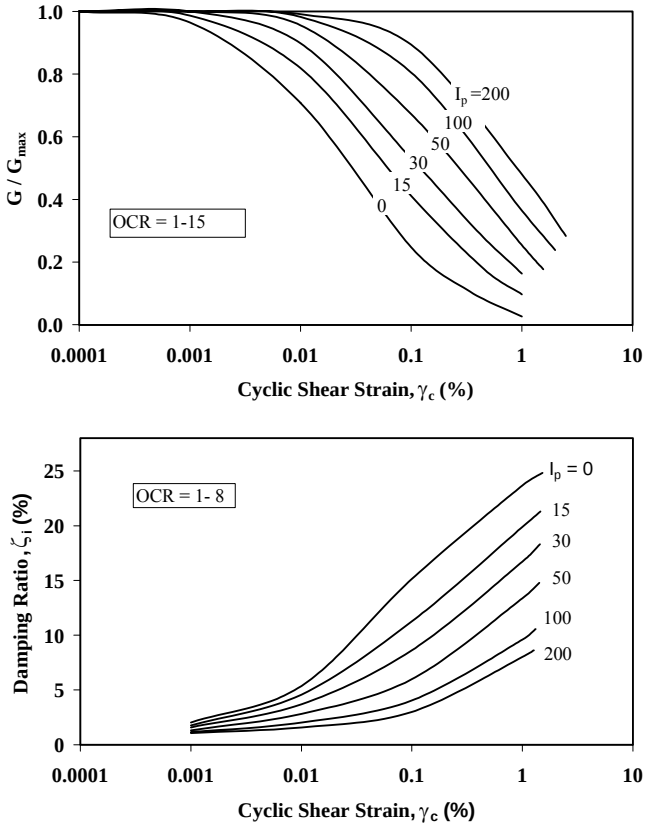

Figure D-2
Relations between G/G_{max} and cyclic shear strain amplitude γ_c for various plasticity indexes I_p

D.3 Soil damping

D.3.1 The soil damping is generally dependent on the dynamic loads acting on the soil. Two different types of soil damping mechanisms can be distinguished:

— material damping associated with hysteresis taking place close to the yield zone in contact with the pipe
— radiation damping associated with propagation of elastic waves through the yield zone.

D.3.2 The radiation damping may be evaluated from available solutions for elastic soils using relevant soil modulus reflecting the soil stress (or strain) levels. The radiation damping depends highly on the frequency of the oscillations, and is more important for high frequency oscillations. Soil damping for free spanning pipelines is normally governed by soil material damping.

D.3.3 The case specific modal soil damping ratio, ζ_{soil}, due to the soil-pipe interaction may be determined by:

$$\zeta_{soil} = \frac{1}{4\pi f_0}\left(\frac{\int_L c(s)\phi^2(s)ds}{\int_L m(s)\phi^2(s)ds}\right)$$

where the soil damping per unit length, c(s), may be defined on the basis of an energy balance between the maximum elastic energy stored by the soil during an oscillation cycle and the energy dissipated by a viscous damper in the same cycle.

The equation may be solved from an FEM analysis of the pipe modelled with discrete soil supports. The viscous damping coefficient c_i of support no. i can be calculated from:

$$c_i = 2 \cdot \zeta_i \frac{k_i}{\omega}$$

where

k_i The linearised spring stiffness at support no. i
ζ_i The damping ratio representing support no. i
ω The angular frequency of the mode considered

Knowing the non-linear hysteretic reaction of a support length the damping ratio representing the support can be calculated as

$$\zeta_i = \frac{1}{4\pi} \cdot \frac{E_{Dissipated}}{E_{Elastic}}$$

where

$E_{Dissipated}$ The energy dissipation at support no. i, as illustrated on Figure D-3.
$E_{Elastic}$ The equivalent elastic energy at support no. i, as illustrated on Figure D-3.

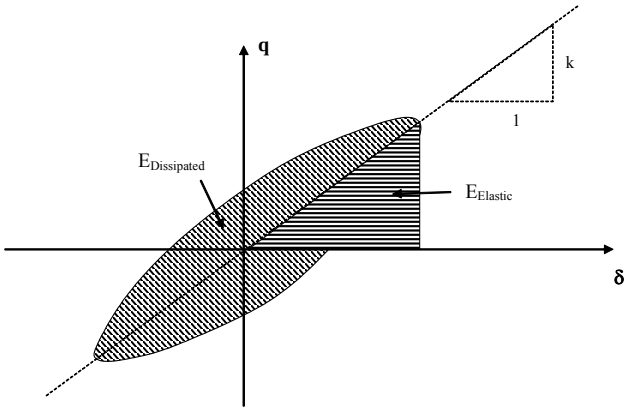

Figure D-3
Energy dissipation at soil support

Because of the soil non-linearity the equivalent spring stiffness as well as the damping ratio are dependent on the displacements at the support. For a case specific determination of the modal soil damping ratio this shall be taken into account. An iterative solution will be required to assure compatibility between:

— the dependency of the mode-shape on the equivalent support springs
— the dependency of the oscillation amplitude on the modal damping
— the dependency of the equivalent springs and the damping ratio of the discrete soil supports on the cyclic support displacements
— the dependency of the modal damping ratio on mode-shape and on support springs and damping ratio.

As basis for the iterations non-linear relationships for spring stiffness, k_i, and damping ratio, ζ_i, as function of pipe penetration and cyclic displacements for the relevant soil and pipe diameter are required. Such relationships are qualitatively shown in Figure D-4, and may be determined either experimentally or analytically. The stiffness relationship connects the part of the response governed by small strain stiffness with the part governed by strength. For an analytical approach the soil shear modulus and material damping as function of cyclic strain and the plasticity index, I_p, as shown in Figure D-2 may be used.

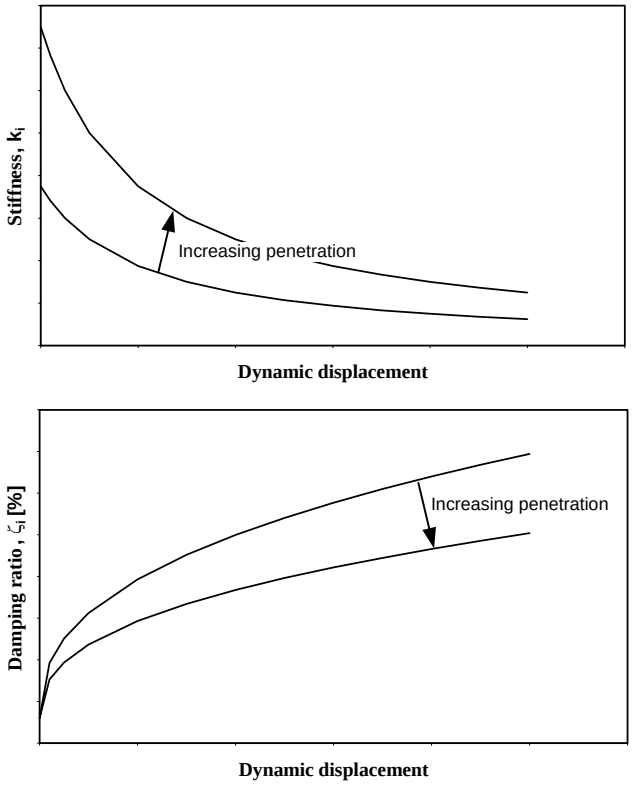

Figure D-4
Nonlinear characteristics of soil support stiffness and damping